



Spatio-temporal variations of lateral and atmospheric carbon fluxes from the Danube Delta

Marie-Sophie Maier^{1,2}, Cristian R. Teodoru¹, Bernhard Wehrli^{1,2}

5 ¹Institute of Biogeochemistry and Pollutant Dynamics, ETH Zürich, Zürich, 8092, Switzerland

²Eawag, Swiss Federal Institute of Aquatic Science and Technology, Kastanienbaum, 6047, Switzerland

Correspondence to: Marie-Sophie Maier (marie-sophie.maier@usys.ethz.ch)



Abstract

- 10 River deltas with their mosaic of ponds, channels and seasonally inundated areas act as the last continental hotspots of carbon turnover along the land-ocean aquatic continuum. There is increasing evidence for the important role of riparian wetlands in the transformation and emission of terrestrial carbon to the atmosphere. The considerable spatial heterogeneity of river deltas, however, forms a major obstacle for quantifying carbon emissions and their seasonality. While river reaches crossing the delta can serve as reference systems, delta lakes are often dominated by aquatic production and channels act as collection systems
- 15 for carbon exported from adjacent wetlands. In order to quantify carbon turnover and emissions in the complex mosaic of the Danube Delta, we conducted monthly field campaigns over two years at 19 sites spanning river reaches, channels and lakes. Here we report greenhouse gas fluxes (CO_2 and CH_4) from the freshwater systems of the Danube Delta and present the first seasonally resolved estimates of its freshwater carbon emissions to the atmosphere. Furthermore, we quantify the lateral carbon transport of the Danube River to the Black Sea.
- 20 We estimate the delta's CO_2 and CH_4 emissions to be 65 GgC yr^{-1} , of which about 8% are released as CH_4 . The median CO_2 fluxes from river branches, channels and lakes are 25, 93 and $5.8 \text{ mmol m}^{-2} \text{ yr}^{-1}$, respectively. Median total CH_4 fluxes amount to 0.42, 2.0 and $1.5 \text{ mmol m}^{-2} \text{ yr}^{-1}$. While lakes do have the potential to act as CO_2 sinks in summer, they are generally the largest emitters of CH_4 . Small channels showed the largest range in emissions including a CO_2 and CH_4 hotspot sustained by adjacent wetlands. The channels thereby contribute disproportionately to the delta's emissions considering their limited surface
- 25 area. In terms of lateral export, we estimate the net export of the Danube Delta to the Black Sea to about 160 GgC yr^{-1} , which only marginally increases the carbon load from the upstream river catchment (8490 GgC yr^{-1}) by about 2 %. While this contribution of the delta seems small, deltaic carbon yield ($45.6 \text{ gC m}^{-2} \text{ yr}^{-1}$, net export load/surface area) is about 4-fold higher than the riverine carbon yield from the catchment ($10.6 \text{ gC m}^{-2} \text{ yr}^{-1}$).

1 Introduction

- 30 In an attempt to improve global climate models, the role of rivers, their deltas and estuaries in the carbon cycle is receiving increasing attention since more than a decade (IPCC, 2007). Back then, the perception shifted from rivers as mere lateral conduits of particulate and dissolved carbon species to an “active pipe” concept, where rivers are considered efficient biogeochemical reactors with the potential to release significant amounts of carbon as CO_2 and CH_4 directly to the atmosphere (Cole et al., 2007; IPCC, 2013). A multitude of global upscaling studies (e.g. Tranvik et al., 2009; Regnier et al., 2013;
- 35 Raymond et al., 2013) estimated the riverine and lacustrine fluxes of CO_2 and CH_4 to the atmosphere on a persistently fragmentary database considering spatial and temporal coverage, especially of headwater streams and large lowland rivers (Hartmann et al., 2019; Drake et al., 2018).

- Along the land-ocean-aquatic continuum, about $0.9\text{--}0.95 \text{ PgC yr}^{-1}$ are estimated to be transferred laterally by rivers to the ocean (Regnier et al., 2013; Kirschbaum et al., 2019). Half of the carbon exported to the ocean is in the form of dissolved inorganic carbon (DIC), while the other half consists of particulate and dissolved organic carbon (POC and DOC) in about
- 40



equal shares (Li et al., 2017; Kirschbaum et al., 2019). Recent estimates suggest that about 50 to >70 % of the carbon inputs from terrestrial ecosystems degas as CO₂ and CH₄ along the way to the ocean (Drake et al., 2018; Kirschbaum et al., 2019), making this the most important export flux of terrestrial carbon from inland waters. While rivers could emit 0.65–1.8 PgC yr⁻¹ (Lauerwald et al., 2015; Raymond et al., 2013), lakes and reservoirs could add another 0.3–0.58 PgC yr⁻¹ (Raymond et al.,
45 2013; Holgerson and Raymond, 2016). Earlier works on inner estuaries, salt marshes and mangroves estimate their contribution to another 0.39–0.52 PgC yr⁻¹ (Borges, 2005; Borges et al., 2005). River deltas and estuaries therefore seem to contribute about equally to CO₂ and CH₄ emissions as lakes and reservoirs, despite representing only about 1/6 of their global surface area (Cai et al., 2013; Holgerson and Raymond, 2016).

50 Deltas and estuaries represent hot spots of carbon turnover and CO₂ and CH₄ emissions due to high nutrient load, large productivity and seasonal flooding. However, differences in geomorphology, anthropogenic alterations, complex hydrology and the influence of tides are just a few of the factors which make it very difficult to compare different deltaic and estuarine systems amongst each other (Galloway, 1975; Postma, 1990). Dürr et al. (2011) attempted to classify this diverse group of coastal habitats, which led to lower global emission estimates of 0.27±0.23 PgC yr⁻¹ of CO₂ and 0.0018 PgC yr⁻¹ of CH₄
55 (Laruelle et al., 2010; Borges and Abril, 2011). These studies, however, did not explicitly consider deltas and inner estuaries of large rivers such as the Amazon, Changjiang, Congo, Zambezi, Nile, Mississippi, Ganges or the Danube.

The close connection of river deltas to adjacent wetlands has the potential to fuel CO₂ and CH₄ emissions. Almeida et al. (2017) show that peak concentrations of CO₂ in the Madeira River, a tributary to the Amazon, are linked to extreme flood events and riparian wetlands in the Amazon basin have been identified as significant sources for the outgassing of terrestrial
60 carbon in the form of CO₂ (Richey et al., 2002; Mayorga et al., 2005). While wetlands are estimated to contribute 1.1 PgC yr⁻¹ (Aufdenkampe et al., 2011) to the global carbon emissions, Amazonian wetland emission alone could contribute another 0.2 PgC yr⁻¹ (Abril et al., 2014). Specifically, riparian systems in the lowlands could provide significant lateral carbon inputs (Sawakuchi et al., 2017). While the lower river basins of Amazon, Mississippi and Zambezi have been subject to CO₂ and CH₄ evasion studies (Sawakuchi et al., 2014; Dubois et al., 2010; Teodoru et al., 2015), others such as Nile and Danube remained
65 uncharted territory in that respect. Both Nile and the Danube River represent one end of the river delta spectrum since they show little exposure to tidal action. Therefore, these deltas experience seasonal flooding, instead of (semi)-diurnal flooding determined by tidal action. We anticipate seasonal variability in CO₂ and CH₄ emissions and in lateral carbon transport to the ocean because of this hydrological regime.

70 In this study, we estimate delta-scale atmospheric CO₂ and CH₄ emissions for the Danube Delta, as well as the lateral carbon transport of the Danube River to the Black Sea. We hypothesized that the hydromorphology of the different waterscapes would influence the outgassing behavior of greenhouse gases by governing gas exchange and biogeochemical processes. The resulting differences in atmospheric fluxes would require treating the waterscapes separately in the upscaling process. Furthermore, we anticipated the seasonality of the flooding to affect both atmospheric and lateral fluxes.



75 To capture this spatial and temporal variability, we conducted a systematic study covering 19 sites in the Danube Delta over
two years with monthly sampling intervals. Based on this time series, we address the systematic differences between the delta's
main waterscapes (river branches, channels and lakes) to classify different open-water sources for greenhouse gas emissions
and dominating biogeochemical processes. Furthermore, we estimate lateral and atmospheric carbon fluxes considering the
spatio-temporal variability, discuss uncertainties linked to the upscaling process and compare the estimates to other major river
80 systems.

2 Methods

2.1 The Danube Delta

The Danube Delta is the second largest river delta in Europe after the Volga Delta. It is located on the Black Sea coast in
eastern Romania and southern Ukraine (Fig. 1). Close to the city of Tulcea, the Danube River splits and forms the Chilia,
85 Sulina and Saint George branch (romanian: Sfantu Gheorghe). In the vast wetland area between the main river sections, the
seasonal floods maintain an aquatic mosaic of reed stands and more than 300 shallow through-flow lakes of different sizes,
which are hydrologically connected to the Danube via natural and artificial channels (Oosterberg et al., 2000). Since 1998, the
Danube Delta has been a UNESCO Biosphere Reserve with nearly 10% strictly protected area and another 40% of the total
surface area declared as buffer zones (UNESCO, 2019). While five of the larger lakes of the Danube Delta have been subject
90 to CO₂ and CH₄ evasion studies in the past (Durisch-Kaiser et al., 2008; Pavel et al., 2009), the main branches of the river and
the small channels are uncharted territory with respect to CO₂ and CH₄ concentrations and fluxes.

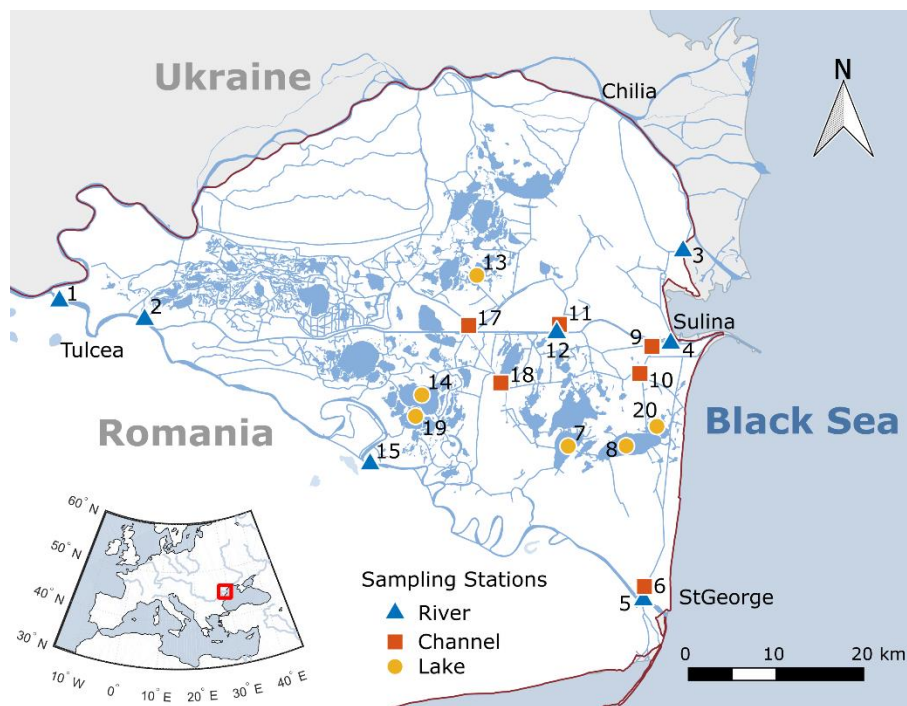


Figure 1 Sampling stations in the Danube Delta, Romania. Near Tulcea, the Danube River splits into three branches: Chilia, Sulina and St. George. Station 16 not shown due to limited access. Shape files for map creation in QGIS adapted from mapcruzin.com (Contains information from www.openstreetmap.org, which is made available here under the Open Database License (ODbL), <https://opendatacommons.org/licenses/odbl/1.0/>).

Hydrology

The hydrology of the Danube River, which drives water exchange with the delta, has a pronounced seasonality. Receiving meltwater from the Alps and Carpathians, the Danube shows peak discharge in spring from April to June (Fig. 2), whereas the discharge minimum occurs in autumn from September through November. December and January often show a small peak in discharge. The discharge provided by the Danube River drives the seasonal and annual hydrological changes in the delta. From 2000 to 2014, the Danube's average annual discharge was $6760 \text{ m}^3 \text{ s}^{-1}$ (ICPDR, 2018), which is a 3 % increase compared to the period from 1930 to 2000 (Oosterberg et al., 2000). In the delta region, the discharge splits into the different main branches as follows: Chilia: 53 %, Sulina: 27 %, Saint George branch: 20 % (ICPDR, 2018). Approximately 10 % of the Danube's total discharge ($620 \text{ m}^3 \text{ s}^{-1}$, averaged 1981-1990) flows through the delta, of which about 20 % ($120 \text{ m}^3 \text{ s}^{-1}$) is lost via evapotranspiration (Oosterberg et al., 2000).

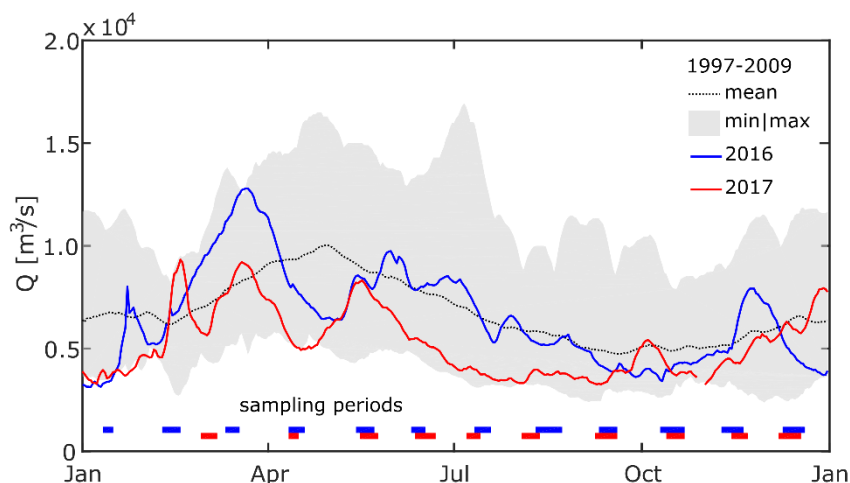


Figure 2 Daily average discharge close to the apex of the Danube Delta. The dotted line and the shaded area show mean and minimum to maximum daily discharge, respectively, for the period from January 1997 to October 2009 at Reni (ICPDR, 2018). Blue and red lines show daily average discharge at Isaccea in 2016 and 2017 (INHGA, 2017; Feodorov, 2017). Horizontal bars indicate the timing of sampling campaigns. X-axis ticks indicate date 15 of the respective month.

110

To assess the hydrological conditions during the time of observation with respect to the long-term average, we compared water level observations from Isaccea (INHGA, 2017; Feodorov, 2017) to the discharge data set from Reni (ICPDR, 2018). Reni is located about 30 km upstream of Isaccea, without any major tributary joining in between. Water level data from Isaccea was converted to discharge using rating curves created from paired water level and discharge data from the National Institute of Hydrology and Water Management (INHGA, 2017). The comparison shows that 2016 was quite an average year in terms of discharge (Fig. 2), while, contrastingly, the Danube had very low discharge in 2017, especially during the period between March and October. Average discharge in 2017 was $5237 \text{ m}^3 \text{ s}^{-1}$, or 23 % below the average flow calculated from the ICPDR data set, hence we refer to it as “dry year”. Water temperature and conductivity of our sampling period were also in general comparable with data from the ICPDR’s long-term monitoring (see SI). Although water temperature measured during summer months in both 2016 and 2017 was up to 3°C warmer than the long-term mean, these values did not exceed maximum temperatures measured in the last 20 years.

115

120

Categorization into river branches, channels and lakes

We categorized our sampling stations into three groups based on geomorphological characteristics: main river branches, lakes and channels. River branch stations are all located along the three main branches of the Danube River exhibiting velocities of about 0.75 m s^{-1} (Danube Commission, 2018), large hydraulic cross-section and frequent embankment. The category lakes refers to shallow (2-3.5 m) open-water bodies within reed bed areas, and 5 out of 6 sampling stations showed abundant macrophytes in summer. Natural and artificial channels represent the third category. They provide a surface water connection between the lakes and the river branches. We included old meanders of the Danube as well as small channels within the Delta. Both of these features show a low flow velocity of up to 0.3 m s^{-1} , yet span quite a range in terms of surface area and depth.

125



130 Accessibility by motor boat determined the sampling stations in lakes and channels and restricted our monitoring to deeper lakes and larger channels. Both lakes and channels are connected to adjacent reed beds and marsh areas. Very shallow or isolated lakes, which are not represented in our data set, may receive a significant part of their water from adjacent reed beds (Coops et al., 2008) and have a higher residence time of up to 300 days compared to the investigated lakes, which have an estimated residence time of 10 – 30 days (Oosterberg et al., 2000).

135 **2.2 Sampling**

Our research area was located in the southern part of the delta enclosed by the Sulina and Saint George branches, which we studied intensively in 2016 and 2017. We focused on the southern part of the Delta, since it is less impacted by agriculture compared to the area north of the Sulina branch (Niculescu et al., 2017). Samples and in-situ measurements were taken once per month at 19 stations (Fig. 1), representing river main branches (n = 7), channels (n = 6) and the larger delta lakes (n = 6).

140 The sampling stations in the channels and lakes cover both the fluvial (west of station 18, Fig. 1) and the fluvio-marine parts of the delta. In-situ measurements and sampling with a Niskin bottle was carried out 50 cm below the water surface. Sample analyses were conducted at the Eawag laboratories in Switzerland.

2.3 Dissolved and particulate carbon species

Samples for DIC measurements were filtered sterile (0.2 μm) and bubble-free into 12 mL Labco Exetainers and stored cool and dark until analysis using a Shimadzu TOC L Analyzer. For the analysis of POC and DOC, water was filtered through 7 μm pre-combusted and pre-weighed Hahnemühle GF 55 filters. The filters were stored at -20°C until analysis, when they were dried and weighed for total suspended matter, subsequently fumigated with HCl for 24 hours to remove the inorganic fraction and analyzed by EA-IRMS (elemental analyzer) for organic carbon content, which we used to calculate POC. The filtered water was acidified using 100 μL 10 M HCl and stored dark at 4°C until analysis of DOC using a TOC L Analyzer (Shimadzu).

150 Due to potential contamination during sampling, DOC data prior to May 2016 was discarded.

2.4 Dissolved gases

2.4.1 Concentration measurements

We used mostly field-based methods for the analysis of dissolved CH_4 , CO_2 and O_2 . In 2016, samples for CH_4 analysis were taken for laboratory-based analysis by gas chromatography. Water was filled bubble-free into 120 mL septa vials by allowing overflow of approximately 3 times the sample volume before preserving the sample by adding CuCl_2 . Depending on the expected concentrations, a headspace of 15-25 mL was created in the lab using pure N_2 . Samples were equilibrated overnight at 23°C on a shaker and the headspace was analyzed using gas chromatography (GC-FID, Agilent Technologies, US). In 2017, we used 1 L Schott-Bottles to prepare headspace equilibration directly in the field using air. Samples were transferred to gasbags and analyzed in the field for CH_4 using an Ultraportable $\text{CH}_4/\text{N}_2\text{O}$ analyzer (Los Gatos Research, LGR). We corrected

155



160 for atmospheric contamination during the processing by subtracting the amount of CH₄ introduced with the air during
equilibration. As tests showed that there was no significant difference between the lab- and field-based methods, we pooled
the data in our analysis. CO₂ concentrations were measured in the field using syringe-headspace equilibration of 30 mL
sampling water with 30 mL air. The syringes were shaken for 2 minutes and allowed to equilibrate before transfer of the
headspace into a dry syringe and analysis in an infrared gas analyzer (EGM-4, PP-Systems). The method is explained in more
165 detail in Teodoru et al. (2015).

Dissolved O₂ concentration was measured in-situ using an YSI ODO probe. The sensor was calibrated daily using water-
saturated air and crosschecked with oxygen readings from an YSI PROPlus multimeter sensor. We measured local in-stream
respiration rates to evaluate if community respiration could sustain our measured CO₂ fluxes. The respiration rate was
measured as O₂ drawdown over a 24 hour period. For the measurement, six BOD bottles were filled with water sample and
170 three were measured immediately afterwards at t = 0. The other three bottles were stored in dark at approximately in-situ
temperatures and O₂ concentration was measured after 24 hours. The respiration rate was derived from the time and
concentration difference, assuming a linear decrease over time. We used this respiration rate to estimate local CO₂ production
rate by assuming a 1:1 aerobic respiration relation of O₂:CO₂. Ward et al. (2018) argue that respiration rate measurements in
BOD bottles are underestimating respiration rate because microbial processes are limited by both the bottle size and the lack
175 of turbulence and suggest a correction factor of 2.7 to correct BOD derived respiration rates for size effects only or a factor of
3.7 for size and low turbulence effects. Applying these correction factors did not change the main point of our comparison
between fluxes and CO₂ production rate.

2.4.2 CO₂ and CH₄ flux measurements

CO₂ and CH₄ fluxes were measured using a floating chamber. The chamber had an internal area of 829.6 cm² and an internal
180 volume of 10080 cm³, leading to a Volume/Area ratio of 12.15 cm. An aluminum foil coating minimized heating during
deployment. CO₂ was routinely measured in the field over a 30-minute period by coupling an infrared gas analyzer (EGM-4,
PP Systems) to the chamber in a closed loop. In 2016, CH₄ was sampled from the chamber by syringe and transferred overhead
into 60 mL septa vials that had been pre-filled with saturated NaCl solution until the liquid was replaced by gaseous sample.
These discrete samples for lab analysis were taken at time t = 0, 10, 20 and 30 min and analyzed by GC-FID. In 2017, this
185 laborious procedure was replaced by attaching the LGR directly to the floating chamber.

Flux chamber measurements were conducted unless conditions were too windy or boat traffic was too frequent in the main
channel. In total, we took 265 flux measurements for CO₂ and 122 for CH₄. Of the latter, 91 measurements seemed to be
without significant influence of ebullition (i.e. R² of linear regression > 0.96, for more detail see SI) and are henceforth referred
to as *diffusive* CH₄ fluxes. In the high-resolution LGR time series, the influence of gas bubbles could easily be identified. We
190 calculated the diffusive flux by fitting a linear regression to periods where data showed no influence of ebullition. In this case,
the flux is calculated from the slope and the height of the gas volume in the chamber. In the discrete time series, it was hard to
distinguish between diffusive flux and ebullition. When the linear regression of the discretely measured samples had an R² <



0.96, we considered the flux measurement to be influenced by bubbles. In this case, we calculated the total flux by dividing the total concentration increase by the observation time, as we did to calculate the total flux of the LGR measurements. Three cases with $R^2 > 0.96$ showed fluxes $> 20 \text{ mmol m}^{-2} \text{ d}^{-1}$ and were therefore also classified as total flux. Discrete time series showing a non-monotonous course ($n = 12$) were excluded from further processing. Missing monotony can have several explanations including sampling captured a bubble or a sample mix up.

Calculation of k_{600}

We used our CO_2 flux measurements to calculate the gas transfer coefficient k_{600} as follows

$$k_{\text{CO}_2} = \frac{F_{\text{CO}_2}}{(p_{\text{CO}_2, \text{water}} - p_{\text{CO}_2, \text{air}}) \cdot K_{\text{H}, \text{CO}_2}} \quad (1)$$

$$k_{600} = \frac{k_{\text{CO}_2}}{(Sc_{\text{CO}_2}/600)^{-\frac{1}{2}}} \quad (2)$$

Where F_{CO_2} is the flux of CO_2 , p_{CO_2} is the measured partial pressure of CO_2 in water and air, respectively, and $K_{\text{H}, \text{CO}_2}$ is the Bunsen coefficient for CO_2 according to Weiss (1974). Sc_{CO_2} is the Schmidt number for CO_2 calculated based on temperature (Wanninkhof, 1992). We estimated missing flux measurements using the median k_{600} of the respective water type and the measured CO_2 concentrations.

Analogously, diffusive CH_4 fluxes were estimated from the individually calculated k_{600} using the Bunsen coefficient from Wiesenburg and Guinasso Jr (1979), the mean global atmospheric CH_4 mole fraction of 1.84 ppm (Nisbet et al., 2019) and the Schmidt number for CH_4 from Wanninkhof (1992). We attributed the difference between this estimate and the total measured flux to ebullition.

2.5 Upscaling atmospheric fluxes to delta-scale

Spatial upscaling of heterogeneous and scarce data is very difficult and handled in various ways in the literature. Like other authors in a global context (Aufdenkampe et al., 2011; Raymond et al., 2013), we believe that median fluxes give a more reliable representation of the fluxes in systems with large gradients. Based on the different characteristics of the three waterscapes, we estimated the delta-scale atmospheric CO_2 and CH_4 fluxes by multiplying the median flux of each waterscape with its respective area (Table 1). We did this for each month separately and summed up the results considering the respective number of days per month.

$$F_{RCL} = \sum_{m=1}^{12} F_{m, RCL} \cdot \vec{A}_{RCL} \cdot 10^3 \cdot \vec{n}_{days, m} \quad (3)$$

$$F_{tot} = \sum_{RCL=1}^3 F_{RCL} \quad (4)$$



220 $F_{m,RCL}$ therefore represents a 12x3 matrix with the median fluxes measured in all months in the three different waterscapes in
 mmol m⁻² d⁻¹. \vec{A}_{RCL} is a row vector with the areas of the waterscapes in km² (see Table 1) and $\vec{n}_{days,m}$ is a column vector with
 the number of days of each month. We converted the resulting annual flux F_{RCL} per waterscape in mol yr⁻¹ to GgC yr⁻¹ and
 GgCO₂eq yr⁻¹, the latter assuming a global warming potential for CH₄ of 28 over 100 years, i.e. neglecting climate feedbacks
 (IPCC, 2013). Summing over the three sub-systems, we arrived at the total water-air flux in the delta (F_{tot}). We also performed
 225 this calculation using 25- and 75-percentile instead of the median to assess upper and lower boundaries of our estimate.

For a reliable upscaling of fluxes, we determined the surface area of each waterscape as precisely as possible (Table 1). We
 estimated the area covered by the Danube's branches by refining publicly available shape files for Romania and Ukraine
 (mapcruzin.com, 2016a) using the "Open layers plugin" in QGIS, which allowed comparison of the shape file with satellite
 230 images. We used the same procedure for the lakes and arrived at the surface area reported by Oosterberg et al. (2000).
 Assessment of the surface area of the delta channels was more difficult, as many of the small channels are hard to identify on
 satellite images. Generally, estimating the width of the channels is challenging due to emergent macrophyte coverage, which
 depending on image quality blends in with adjacent reed. Instead of mapping the channels, we therefore used the overall
 channel length reported by Oosterberg et al. (2000) and assumed an average channel width of 10 m, which means the resulting
 235 surface area is on the lower end. Especially the old meanders of the Danube (Dunear Veche) do have a much higher range of
 100–200 m.

240 **Table 1 Surface area of Danube Delta features. Assuming 10 m channel width means the estimation of the surface area of the
 channels is on the lower end. The surface areas of freshwater and wetland do not add up to the total area, since parts of the delta
 are covered by forest and agricultural polders.**

Feature	Area [km ²]	Source
Freshwater	455	Sum of river branches, channels and lakes
- River branches	164	Extracted using QGIS*
- Channels	33	Length of canals and partially modified streams from Oosterberg et al. (2000); 10 m width assumed.
- Lakes	258	Oosterberg et al. (2000) & extracted using QGIS*
Wetland	3670	Mihailescu (2006)
- Marsh vegetation (total)	1805	Sarbu (2006)
o Scripo-Phragmitetum	1600	Sarbu (2006)
Agriculture, forest, settlements, pastures, fish ponds	1515	Total surface area – wetland - freshwater
Total surface area within the 3 main branches	3510	Niculescu et al. (2017)



Total surface area of the delta	5640	Mihailescu (2006)
Surface area of the Danube River catchment	817000	Tudorancea and Tudorancea (2006)

* based on shape files adapted from mapcruzin.com (2016a), contains information from www.openstreetmap.org, which is made available here under the Open Database License (ODbL), <https://opendatacommons.org/licenses/odbl/1.0/>.

2.6 Import by Danube River and Export to Black Sea

To compare the delta's CO₂ and CH₄ emissions to the lateral transfer of carbon from the catchment to the Black Sea and the influence of the delta region, we also calculated the loads of dissolved and particulate carbon species transported by the Danube River at the delta apex and close to the Black Sea via Eq. (5) and Eq. (6). Since CH₄ showed much smaller concentrations (~factor 100–1000 with respect to DOC and DIC), we did not include it into the calculation.

$$F_{b,m} = C_{b,m} \cdot \overline{Q_{b,m}} \quad (5)$$

$$F_{tot} = \sum_{b=1}^3 \sum_{m=1}^{12} F_{b,m} \cdot n_{days,m} \quad (6)$$

$C_{b,m}$ is the concentration of DIC, DOC or POC measured in month m in branch b and $\overline{Q_{b,m}}$ is the respective average daily discharge. $F_{b,m}$ is the resulting average flux per day in each month. In a second step, we multiplied the average daily flux by the number of days per month $n_{days,m}$ and took the sum over all months and the 3 different branches. The import of carbon by the Danube River was calculated similarly, only $b = 1$ in this case. We used the data from station 1 (Fig. 1) to estimate how much carbon enters the three main branches and the delta itself. Data from the stations in the three main branches close to the Black Sea (station 3, 4 & 5, Fig. 1) were used to estimate the amount of carbon exported to the Black Sea.

In our data processing, we decided to exclude one unusually high POC value in April at the Sulina branch (station 4) from our load calculation as we assume it is caused by a high discharge, high turbidity event that does not represent the monthly mean well. Instead, we interpolated between March and May. For DOC, we replaced missing data from January to April 2016 by the measurements at the same stations in 2017, assuming that they are also good estimates for the previous year. This way, we arrived at DOC estimates that cover the same period as DIC and POC.

2.7 Statistical analysis

We used Matlab R2016a and R2017b for the statistical analysis of the data set. The data was evaluated for normal distribution using histograms and quantile-quantile-plots. In case of O_{2,sat}, CH₄ and POC, data distribution improved towards normality using log-transformation, however the results were not fully satisfying. Levene's test furthermore revealed the heteroscedastic nature of our data. Results for tests of significant difference between the three aquatic categories from the non-parametric Kruskal-Wallis test (De Muth, 2014) followed by a multiple comparison test after Dunn-Sidak were therefore taken very



cautiously. Given the non-normality of the data, we report median instead of mean values and give ranges as 25 to 75 percentile or minimum to maximum measured value as indicated.

Boxplots shown in this paper are indicating the 25 and 75 percentile, as well as the median. Outliers are detected using the Interquartile range ($1.5 \times \text{IQR}$). The whiskers are indicating the minimum and maximum values that are not detected as outliers
270 by this procedure.

3 Results

3.1 Dissolved and particulate carbon species

DIC concentrations measured during our study ranged from 1.6 to 4.2 mM (Fig. 3a). Median DIC concentrations were around 3.0 mM over the whole observation period, with channels showing 10 % higher and lakes showing 3 % lower median
275 concentrations than the main river. In 2016, concentrations were lowest in August and highest in December in all three groups (Fig. 3b). In 2017, median concentrations were 10 % (rivers) to 20 % (channels, lakes) lower than in 2016.

DOC levels in the delta were about 1.8-times the concentrations observed in the river (Fig. 3c & 3d). Channels and lakes had very similar concentrations and both showed a general increasing trend from May to October 2016 but in the river concentrations already peaked in July 2016 and were lowest in October. Median concentrations were quite comparable for
280 2017, with a tendency towards lower values: DOC in the main river in August 2017 was nearly 30 % lower than in the previous year. Most of the year, DOC concentrations were nearly a factor 10 smaller than measured DIC concentrations.

In 2016, we observed the lowest median POC concentration in the channels (Fig. 3e & 3f). Median concentrations in both rivers and lakes were nearly twice as high compared to channels, but showed a distinctly different seasonality: POC was highest in the main river from March to June, while it peaked in lakes during August to October suggesting different carbon
285 sources.

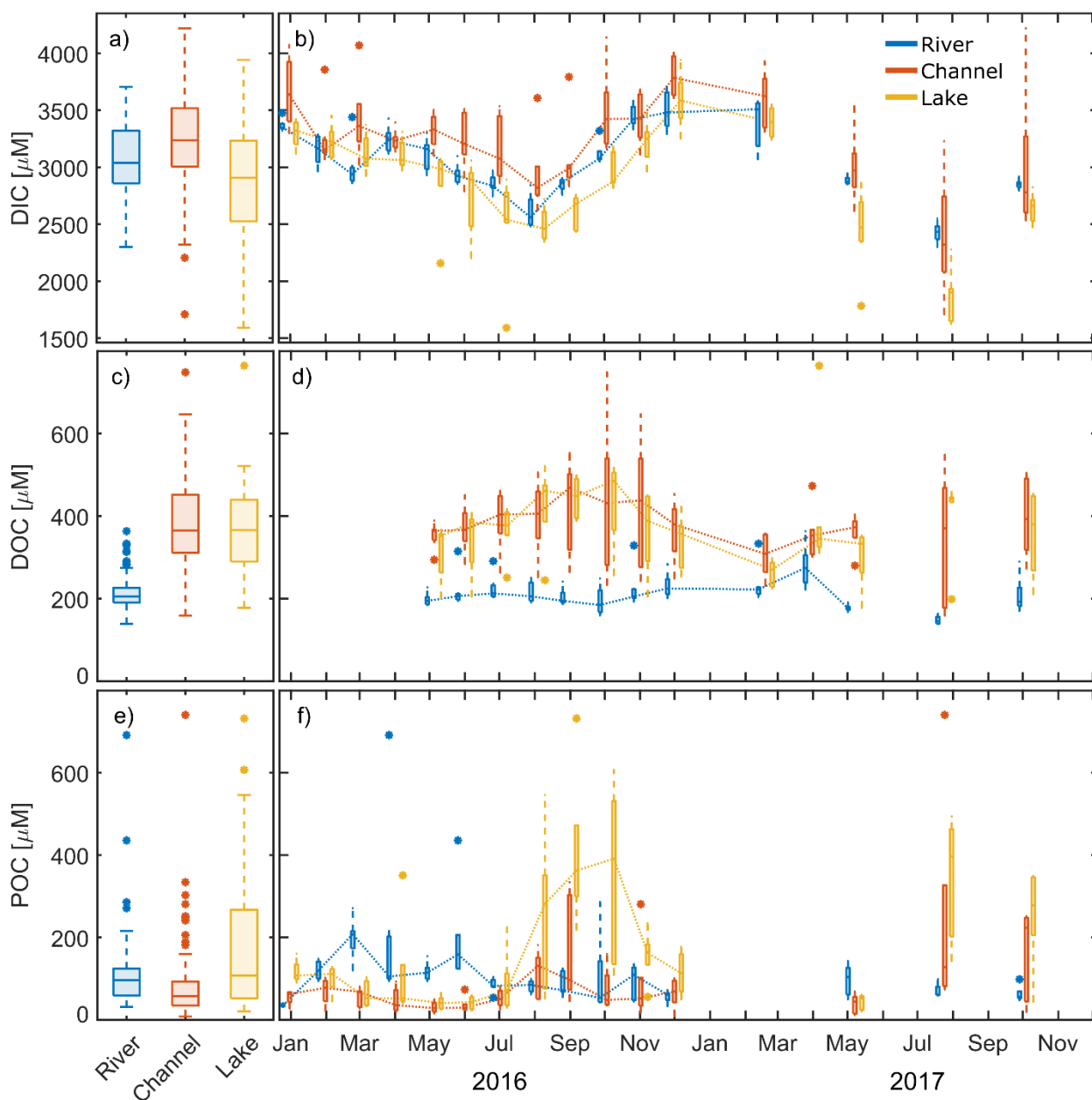


Figure 3 Measured DIC, DOC and POC concentrations in the different waterscapes (river, channel, lake). Left panels (a, c, e): 2-years observation period. Right panel (b, d, f): seasonality of the data. Dotted lines connect median values. X-axis ticks indicate day 15 of the respective month. Boxplots indicate 25 and 75 percentiles, as well as median, whiskers indicate maximum and minimum, with data $> 1.5 \cdot \text{IQR}$ is shown as outliers.

290



3.2 Dissolved gases

3.2.1 Concentrations

During the entire monitoring period, CH₄ in water samples of the delta was always oversaturated with respect to atmospheric
295 equilibrium concentrations of 0.0046 to 0.0023 μM at T = 0 to 30 °C (Fig. 4a & 4b). Median concentrations in the river samples
were thus ~100 times oversaturated (0.33 μM). The channels exhibited a more than 3-times higher median concentration than
the main river (1.1 μM) with highest concentrations in July to September 2016 (up to 59 μM). By contrast, the median
concentration in the lakes exceeded the value of the main river only slightly (0.43 μM), yet with a much larger range. In all
three subsystems, concentrations increased from February 2016 to maximum values in July to October 2016. In 2017,
300 concentrations were lower in the channels compared to 2016.

In analogy to CH₄, we found CO₂ concentrations to be constantly supersaturated with respect to the atmosphere in the main
branches of the Danube, ranging from 26 to 140 μM (Fig. 4c & 4d). The median concentration of 59 μM was more than 3-
times as high as the equilibrium concentration of CO₂ at 15°C (18.2 μM). Channels showed a much higher range (2.4 to
790 μM) with a significantly higher median of 140 μM. During the entire monitoring period, we encountered undersaturated
305 conditions in this class at only two stations (17 and 18) in August 2017. Lakes, however, were undersaturated at 11 occasions
in 2016 and 32 occasions in 2017. Dissolved concentrations in this category ranged from 0 to 95 μM with a median of 28 μM.
In 2016, CO₂ concentration showed a pronounced seasonality in all three subsystems. In the main river, median CO₂ nearly
doubled from January 2016 to April 2016 and subsequently decreased to reach levels around 60 μM. In 2017, no clear seasonal
pattern emerged. That year, median values mostly ranged around 60 μM, with lowest median concentration recorded in June
310 (44 μM) followed by the maximum in July (81 μM).

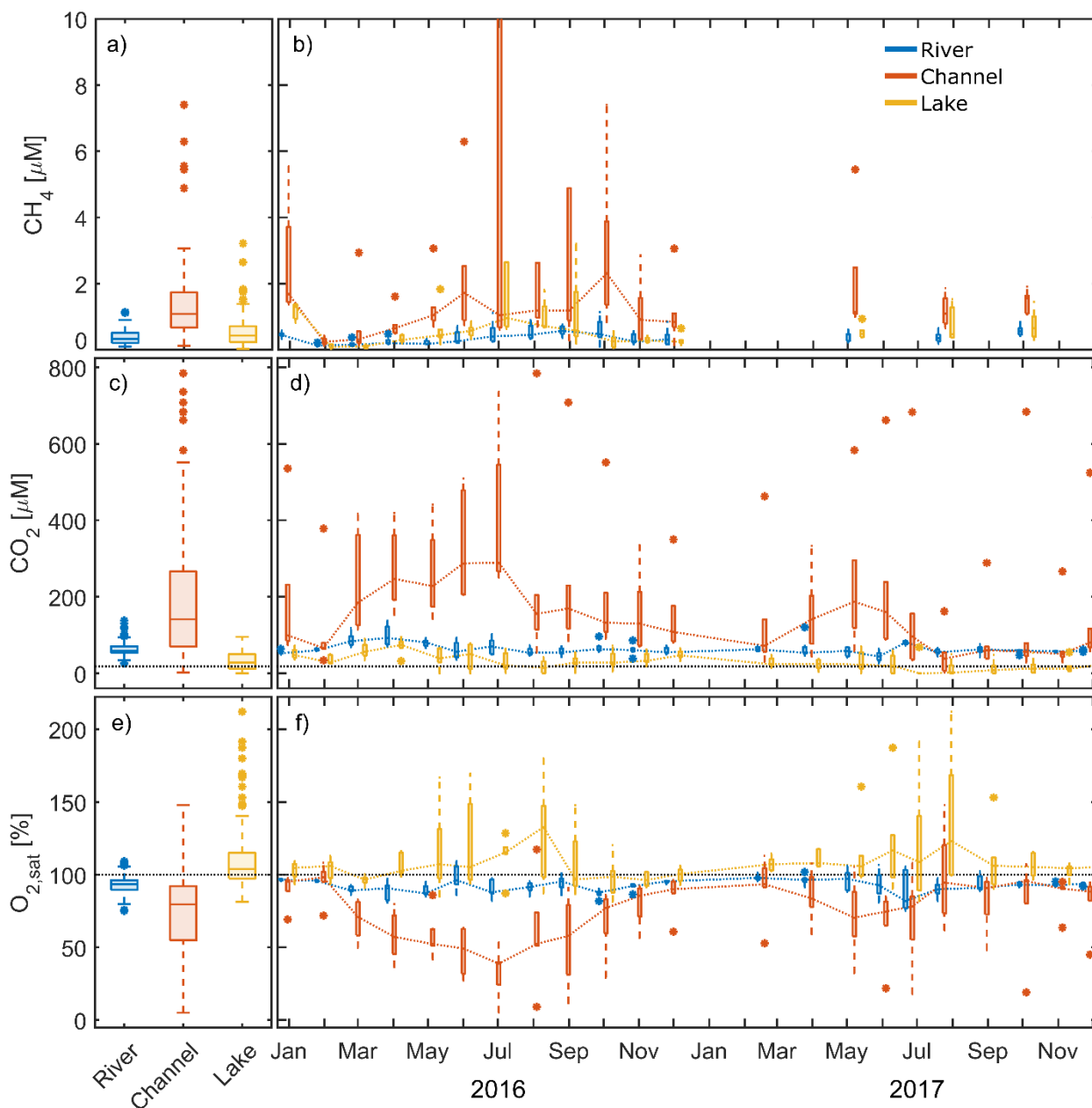
Channels showed the largest increase of CO₂ during the warm season: median concentrations increased more than 4-fold, from
66 μM in February 2016 to 290 μM in July 2016. In terms of inter-annual CO₂ variability, 2017 showed a later and less
pronounced increase in concentration (72 μM in March to 187 μM in May) followed by an earlier decline than 2016. From
August 2017 to November 2017, median monthly concentrations ranged around 50 μM and were lower than the concentrations
315 in the main river during this period. In general, CO₂ concentrations in the channels in 2017 were 18 to 75 % below the values
observed in 2016. We found the highest concentrations in the eastern part of the delta (station 10, Fig. 1), where concentrations
reached around 360 μM in winter and up to 785 μM in summer 2016.

Compared to rivers and channels, lakes generally had the lowest CO₂ concentrations and showed a distinctly different seasonal
pattern. Most of the observed lakes (station 7, 8, 13 and 14) were undersaturated in the period from May to November 2016.
320 CO₂ undersaturation in these lakes (incl. station 20) occurred 3-times more often and over a longer period from March to
December in the dryer year 2017. In 2016, lakes showed highest median CO₂ concentrations in April (74.4 μM) and lowest
concentrations in July and August (20.5, and 14.6 μM, respectively). With the concentration increase in early spring, the
decrease in summer and the following increase in autumn, the seasonal signal in 2016 recalls a sinusoidal curve. The pattern
in the drier year, 2017, however, showed less variation with lower concentrations, which were ranging from 0 to 71 μM.



325 O₂ saturation, as one might expect, often showed a mirror image to the CO₂ time series in all three systems (Fig. 4e & 4f). The main river was generally slightly undersaturated with a median O₂ saturation of 93 %. O₂ saturation in river water ranged between 75 and 109 % during the whole observation period. Median saturation in the channels was 14 % lower (79.5 %) and – as for CO₂ – covered a much broader range than in the main river: lowest values observed were as low as 5 % O₂ saturation (0.4 mg L⁻¹) in July 2016, while maximum saturation reached nearly 150 % in August 2017. In winter, O₂ saturation in the

330 channels was comparable with the river stations. Station 10 showed an exceptional behavior and never exceeded a saturation of 72 % or 9 mg L⁻¹. O₂ saturation in the channels strongly decreased in spring and summer months resulting in concentrations of less than 2 mg L⁻¹ at stations 9 in July 2016 and at station 10 from July to September 2016 and in June, July and October 2017. Contrastingly, most lakes showed a strong oversaturation of up to 180 % from April to October, resulting in a median saturation that slightly exceeded 100 %.



335 **Figure 4** Measured CH_4 and CO_2 concentrations and O_2 saturation in the different waterscapes (river, channel and lake). Left panels
 (a, c, e): pooled data from 2-years. Right panel (b, d, f): seasonal dynamics with dotted lines connecting median values. X-axis ticks
 indicate day 15 of the respective month. a) & b) CH_4 in 2016: four channel values (ranging from 22.2 to 58.0 μM) and one lake station
 (12.5 μM) exceeding 10 μM were cutoff. c) & d) dotted line represents equilibrium concentration of CO_2 at 15°C (18.2 μM). Boxplots
 indicate 25 and 75 percentiles, as well as median, whiskers indicate maximum and minimum, with data > 1.5*IQR is shown as
 340 outliers.



3.2.2 Measured atmospheric CO₂ and CH₄ fluxes

Median CO₂ fluxes were largest in channels (93 mmol m⁻² d⁻¹, see Table 2), where we also observed the highest overall flux of 880 mmol m⁻² d⁻¹. Lakes were the only locations that showed significant negative fluxes, i.e. CO₂ uptake during summer, when O₂ was strongly oversaturated.

345 The highest median diffusive fluxes of CH₄ were observed in the channels with 1.1 mmol m⁻² d⁻¹. Diffusive efflux from the river was generally lowest, while the lakes showed the largest variability with a minimum of 0.03 and a maximum of 6.7 mmol m⁻² d⁻¹. Considerable ebullition occurred only in the delta lakes and channels, which accounted for ~70% of the total CH₄ flux.

350 The gas transfer coefficient, k₆₀₀, was calculated from the measured CO₂ fluxes. Median k₆₀₀ was lowest in in the river branches and in the channels with 0.69 m d⁻¹ and 0.74 m d⁻¹, respectively (see Table S1). As lakes were more exposed to wind, median k₆₀₀ was considerably higher (1.2 m d⁻¹) and we observed the maximum k₆₀₀ of 8.6 m d⁻¹ in this category.

Table 2 Median and range of measured CO₂ and CH₄ fluxes [mmol m⁻² d⁻¹] and calculated k₆₀₀ values [m d⁻¹]. n states the number of measurements. The range indicates minimum and maximum observations.

Parameter	River			Channel			Lake		
	median	range	n	median	range	n	median	range	n
F _{CO2}	25	7.3-150	57	93	-9.7-880	105	5.8	-110-160	103
F _{CH4, tot}	0.42	0.056-2.7	21	2.0	0.062-51	47	1.5	0.031-47	54
F _{CH4, dif} ^a	0.37	0.056-2.7	17	1.1	0.16-6.2	34	0.82	0.031-6.7	40
k ₆₀₀ ^b	0.69	0.20-3.4	57	0.74	0.11-5.4	103	1.2	0.13-8.6	96

^a The data in this table relies only on measured F_{CH4, dif}. Missing diffusive CH₄ fluxes for the upscaling were calculated from k₆₀₀.

^b Measurement uncertainty lead to negative k₆₀₀ values in 9 cases (n_{channel} = 2, n_{lakes} = 7). These values were deleted manually, thus n_{k600} is < n_{F_{CO2}} for channels and lakes.

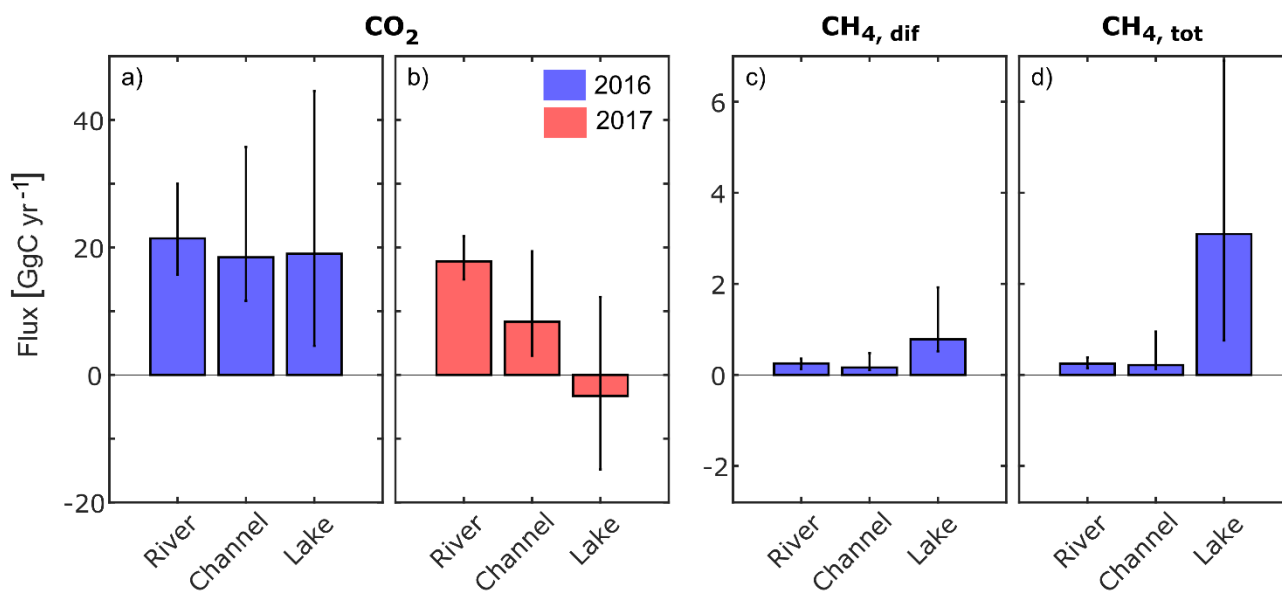
355 3.3 Upscaling atmospheric fluxes to delta-scale

The upscaling of the freshwater CO₂ and CH₄ fluxes to the freshwater surface of the delta according to Eq. (4) led to a net CO₂ flux of 60 GgC in 2016 and less than half (23 GgC) in the drier year 2017 (Fig. 5 and Fig. 7a, case “c”), when the overall contribution of the three compartments was lower and lakes turned into a net sink. The diffusive CH₄ flux (Fig. 7c) was one order of magnitude smaller than the CO₂ flux (Fig. 7a) but it increased 3-fold when ebullition was considered (Fig. 7d).

360 Especially the CO₂ fluxes seem to be subject to considerable inter-annual variability (Fig. 7a & 7b), which highlights the need to discriminate between different years during the upscaling process. It is likely that the different hydrological conditions



triggered different amounts of lateral inflow from the reed-covered wetlands and cause the large variability in CO₂ fluxes. For CH₄, this effect seems to be much smaller.



365 **Figure 5** Annual greenhouse gas fluxes to the atmosphere obtained by upscaling the monthly median flux to the total area of each
waterscape and taking the sum over all months (details see text). Black vertical lines indicate the uncertainty and were calculated
by using the 25 percentile and 75 percentile, respectively, instead of median values for the calculation. CO₂ flux in a) 2016 and b)
2017, c) diffusive and d) total CH₄ flux in 2016. Due to large data gaps, this calculation was not done for CH₄ in 2017. All Fluxes are
in GgC yr⁻¹. A table with the values can be found in the SI.

370

A look into the contribution from the different waterscapes shows that the river branches the main source of CO₂ to the
atmosphere were in both years (Fig. 5a & 5b). Despite their small surface area (7 %), channels contributed 32–37% to the total
CO₂ flux. Lakes on the other hand switch from a net CO₂ source of 19 GgC in 2016 to a small net CO₂ sink of -3.3 GgC in the
drier year 2017. In 2016, the lakes emitted the largest share of CH₄: 66 % considering only diffusive fluxes (Fig. 5c) and 86 %
375 considering total CH₄ fluxes (Fig. 5d). Considering the global warming potential of CH₄ (IPCC, 2013), CH₄ was responsible
for 17% of the total 260 GgCO₂eq yr⁻¹ emitted in 2016.

3.4 Lateral carbon transport

The annual import of carbon to the apex of the Delta amounts to 8490 GgC yr⁻¹ (Fig. 8). This flux consists mostly of inorganic
380 carbon (DIC, 91 %), while DOC and POC comprise only small fractions of 6 and 3 %, respectively. Because of its low
solubility and ~100 to 1000 times lower concentration (DOC and DIC, respectively), we did not include CH₄ into the
calculation. Lateral fluxes are highest in spring, when discharge is highest. About 10% of the Danube's water is channeled



into the delta before reaching the Black Sea (Oosterberg et al., 2000), we thus assume that 10% of the annual carbon load of the Danube reaches the delta (i.e. 849 GgC yr⁻¹).

385 The water export from the delta, however, is poorly constrained. The balance between precipitation minus evaporation is negative, poorly quantified and quite variable. We therefore rely on the flux balance of the three branches to estimate carbon export from the delta. The resulting export to the Black Sea via the Danube's main branches amounts to 8650 GgC yr⁻¹ and is less than 2 % higher than the inflow load reaching the apex of delta. It mainly relates to increased DOC levels reaching the main branches from the delta, especially during the spring flood. The relatively small fraction of water that passes through the delta changes the relative fraction of DOC and POC only marginally to 7 % and 4 %, respectively, while the largest fraction in the water reaching the Black Sea remains DIC (89 %, Fig. 8). POC import from the catchment exceeds the export to the Black Sea in February and March, while DOC import exceeds export only during August (data not shown).

4 Discussion

4.1 The main waterscapes of the Danube delta

395 As we had hypothesized, carbon dynamics differed significantly across the three different waterscapes. The non-parametric Kruskal-Wallis test followed by the Dunn-Sidak test showed that the median of the three classes are significantly different for concentrations of CH₄, CO₂, O₂ and DIC (see SI). In case of DOC, only the rivers differ significantly from the other two groups, while in the case of POC, only channels are significantly different. Rivers and lakes, however, may differ significantly in the quality of their POC, as observed by the seasonality of the signal, which shows that high POC in the river actually occurs during high discharge in spring, while high POC in the lakes occurs during algal blooms in late summer. As a non-parametric test, the Kruskal-Wallis tests does not require normal distribution of the data, but it requires homoscedasticity, i.e. equal variance of the data groups investigated for difference in median. A violation of this requirement could potentially distort the test results (Hedderich and Sachs, 2016). Our observations in the seasonal plots (Fig. 3 & 4), however, support the results of the test: in most cases, the boxplots do not overlap, supporting the notion that the three groups are significantly different. For example, DOC is significantly higher in the delta lakes and channels due to the strong primary productivity of these systems. CO₂ is significantly higher in the channels than in the other two categories, coinciding with significantly lower levels in O₂, which is often driven by lateral exchange with the wetland (Zurbrügg et al., 2012). The large difference between the waterscapes with respect to CO₂ and CH₄ fluxes supports our approach to treat the waterscapes independently when upscaling the flux measurements to the total water surface of the delta.



410 4.2 Dominating processes

4.2.1 River branches

The main river branches of the Danube are mostly influenced by the hydrology and chemistry of the catchment, as shown by the comparison between the concentrations at the delta apex with concentrations in the three main branches close to the Black Sea. There is comparably little variation between the stations with respect to DIC, DOC and POC. At all sites, O₂ is slightly
 415 undersaturated most of the times, but we don't see a strong influence of the delta close to the Black Sea.

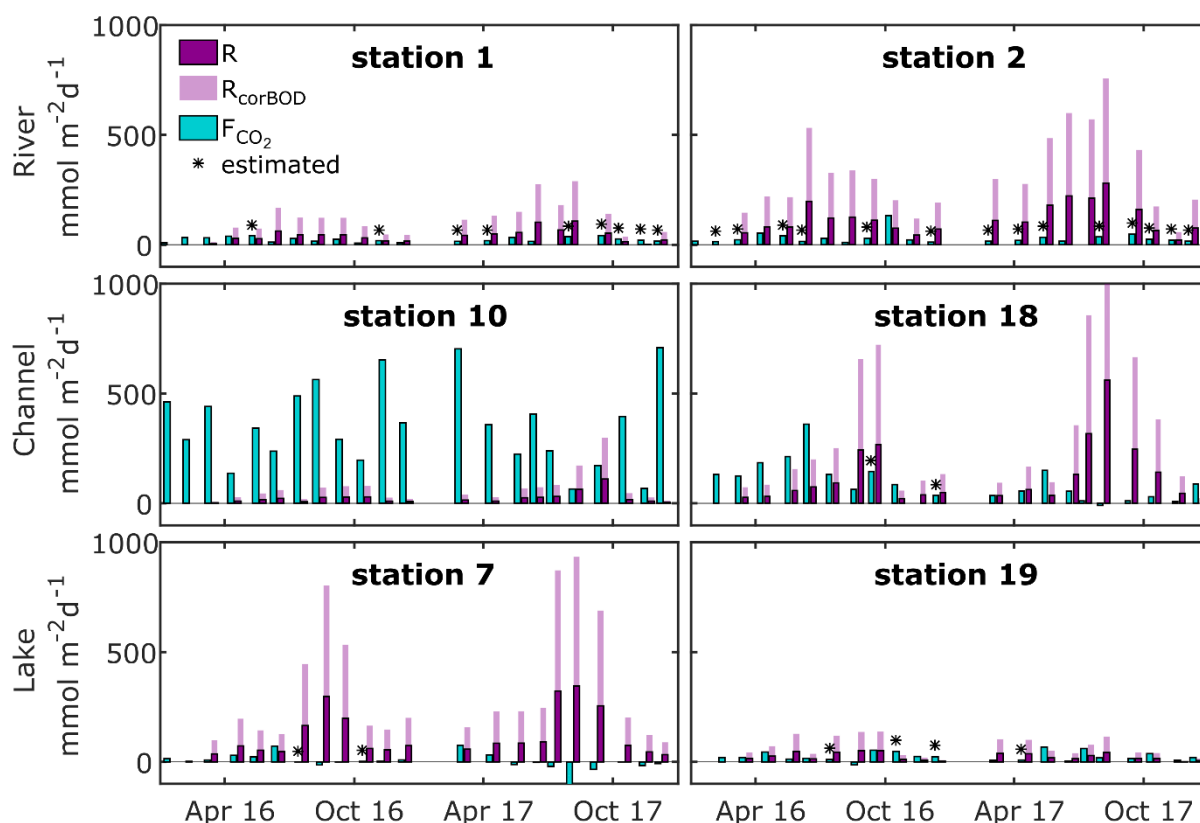


Figure 6 Flux rate and production rate of CO₂ as calculated from O₂ community respiration incubations for selected river, channel and lake stations. Fluxes marked with asterisks were calculated from median k_{600} of our observations in the respective waterscape. Dark purple bars represent measured respiration rates, light purple bars indicate the effect of a correction for measurement limitations using BOD bottles (factor 2.7, see Ward et al. (2018)).
 420

4.2.2 Channels

Carbon dynamics in the channels is strongly affected by the water source. The channels are connecting the river branches to the delta lakes. The direction of this connection depends primarily on hydrologic gradients between the delta and the main branches, which means that flow direction can reverse in individual channels and thus alter their chemical signature due to a
 425 change in the main inflow. Seasonally, the channels transport dissolved carbon into the delta and provide nutrients to the reed



stands during the high-water season. During times of receding water levels in the main branches, the channels act as the delta's drainage pipes. The comparison between CO₂ fluxes and local CO₂ production rates (Fig. 6) shows that the high CO₂ fluxes in the channels are often not sustained by in-stream respiration alone, in contrast to what we observed in the river and lakes. While this discrepancy is mainly occurring during high discharge in spring, it is most evident at station 10, where it occurs
430 throughout the year 2016. Station 10 is located in Canalul Vatafu-Imputita, at the border of a core protection zone of the biosphere reserve. During this study, it stood out as a CO₂ hot spot, responsible for the highest CO₂ concentrations (Fig. 4d). Additional CO₂-rich water inflows from adjacent wetlands could explain the large CO₂ fluxes in excess of CO₂ production. The water at station 10 was always exceptionally clean, low in oxygen content and had a low pH, supporting the hypothesis of a pronounced input from the reed beds. During times of unusually low water levels, such as in August and September 2017,
435 the lateral influx from the reed seems to cease (Fig. 6). The at first glance contradictory timing of increased lateral inflow during increasing water levels at the other channel stations could be explained by a pressure wave: water flooding the vegetated area in the west will push out "old" water with a long residence time in the vegetated area at the other edges further east. In general, channel water in the Danube Delta is therefore a mixture of three main sources: Danube river water, lake water and water infiltrating from the wetland. The importance of the individual water source depends on the location of the channel
440 sampling sites and on the water levels, which trigger flooding or draining conditions.

4.2.3 Lakes

In the lakes, longer residence times of 10–30 days allow primary production and local decomposition of organic matter to become important factors driving carbon cycling. We observed abundant macrophytes like *Ceratophyllum demersum* and *Elodea canadensis* growing in spring and early summer, which, depending on lake depth, even reached the lake water surface.
445 Around July, algal blooms significantly reduced the macrophyte abundance. This pattern seems to be reoccurring due to the eutrophic state of the delta lakes (Tudorancea and Tudorancea, 2006; Coops et al., 2008; Coops et al., 1999). Both macrophytes and algal blooms caused a drawdown of CO₂ and supersaturation of O₂ (Fig. 4d & 4f). The algal blooms also partly explain the peak in measured POC from July to November, which extended to most of the delta's channels (Fig. 3d). The degradation of the macrophyte biomass coincided with locally elevated CH₄ concentrations from July to October (Fig. 4b).
450 In constructed wetlands, macrophytes were found to influence the composition of methanogenic communities by affecting dissolved O₂ and nitrogen in the rhizosphere, which had a direct impact on the amount of CH₄ released to the atmosphere (Zhang et al., 2018). *Potamogeton crispus*, for example, which is also found in the delta lakes and channels, seasonally sustained CH₄ fluxes that were up to 3 times higher than CH₄ fluxes from *Ceratophyllum demersum* (Zhang et al., 2018). Studies showed, that the plant community composition in the delta lakes shifted since the 1980s due to increasing
455 eutrophication, which also lead to an increase in *Potamogeton* species recorded in the delta (Sarbu, 2006). It remains unresolved whether this change in vegetation also affected the CH₄ release in delta.



4.3 Uncertainties linked to the upscaling procedure

4.3.1 Spatial heterogeneity

In a hydrologically complex system like the Danube Delta, upscaling CO₂ and CH₄ is prone to several sources of uncertainties, most of them linked to the delta's small channels and lakes. First, the channel category showed a large range not only in DOC and POC concentrations, but also in dissolved gases and their fluxes. We attribute this primarily to the varying contribution from the three different water sources, with lateral influx from the reed stands drastically increasing local CO₂ concentration and fluxes. One could thus argue that this group is too broad and should be refined. However, in a complex system like the Danube Delta, this is a laborious task, since individual channels are known to reverse flow direction (Irimus, 2006) and potentially also the amount of lateral inflow depends on the hydrologic conditions in the main branches. The existing 1D-hydrological model "Sobek" (DaNUbs, 2005) could assist in delineating periods of reversed flow, but the detailed model for the exchange with the wetlands would have to be developed.

Second, the surface area of the channels is estimated based on the channel length given in Oosterberg et al. (2000) and an assumed channel width of 10 m, which leads to an estimated surface area that we consider quite conservative. More exact mapping or better spatial data, which might exist with local authorities but was not at our disposal, could improve this estimate. A larger or smaller surface area attributed to the channel would influence the flux estimates from this category accordingly.

Third, we identified station 10 as a CO₂ hot spot with concentrations reaching up to 22000 ppm during our study. The hot spot channel had an east to west orientation and was draining a core protection zone. Considering channels with these two criteria indicates potential hot spots could account for up to 2 % of the channel length (see SI) and contribute up to 20 % of the CO₂ and CH₄ fluxes of the channel category. The overall emissions from the channels (incl. hotspot channels) was decreased by 10 to 30% in this scenario, since considering the high fluxes separately lowered the median value used for the calculation of the channel fluxes. A first step to improve the upscaling would thus be to map the spatial distribution of dissolved gases in the delta. This would give insight on important questions linked to the hot spots: How many hot spots did we miss with our discrete sampling approach? What is their lateral extent? And how steep are the concentration gradients between hot spots and nearby sites?

Fourth, our study neglected small, hardly accessible and remote lakes. A study of various-size lakes in northern Quebec revealed a strong, negative relation between lake CO₂ concentration (and fluxes to the atmosphere) and lake area suggesting higher CO₂ emission potential of smaller lakes compared to large-area lakes (Marchand et al., 2009). Previous studies of the small area lakes in the Danube Delta characterize them as very clear-water lakes (Coops et al., 1999) with little or no surface water connection to the main branches (Coops et al., 2008), with increased water residence times and O₂ concentrations below 5 mg L⁻¹ during midday (Oosterberg et al., 2000). This indicated that these lakes, like the hotspot channel in this study, receive the majority of their water from the reed stands (Oosterberg et al., 2000). In contrast to the channels, which are wind sheltered by 2–4 m high reed stands, these small lakes provide a larger surface area and thus a larger wind fetch. Depending on the primary productivity in these lakes, better wind fetch in combination with water contributions from the reed could result in

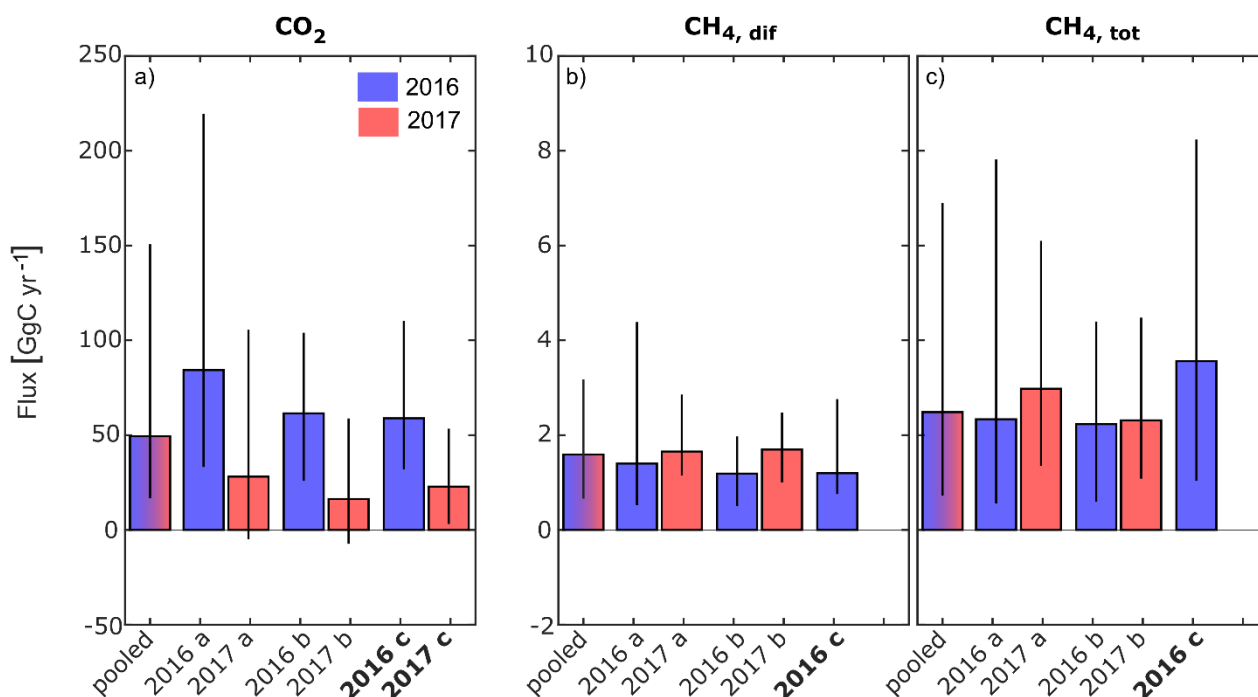


490 higher fluxes to the atmosphere, at least compared to the larger lakes measured in this study. Based on literature research, we estimate the area of potentially isolated lakes to 99 km². Attributing these isolated lakes with channel like flux properties would raise the total CO₂ and CH₄ emissions of the lakes by several fold and turn them from a potential CO₂ sink into a CO₂ source in 2017 (see SI). The scenario as such represents an extreme case, but it highlights the potentially large contribution from small, so far overlooked lakes in the delta.

495 **4.3.2 Seasonality**

Seasonal data coverage is often not sufficient to address the seasonality of the fluxes, which might bias the estimates towards either higher or lower emissions. However, not only underrepresentation of certain seasons or events, also the pooling of the data during the upscaling process influences the resulting estimates. In the following, we look at the effects of data pooling for our 2-year data set by comparing different upscaling approaches. In addition to the approach presented in Eq. (4), where we discriminate by year, month and waterscape (case “c”), we also calculated the yearly fluxes in more simple ways by either pooling all data (case “pooled”), discriminating between years only (case “a”), and by discriminating according to year and waterscape (case “b”). In case “c”, where we considered individual months, data coverage of CH₄ did not allow the calculation for 2017. In all approaches, we treated the reed stands in the wetlands as a terrestrial part of the system, i.e. excluding them from the analysis.

505



510 **Figure 7 Comparison of greenhouse gas fluxes from the deltas freshwaters to the atmosphere obtained by the different upscaling approaches “pooled” and cases “a” (discrimination by year), “b” (discrimination by year and waterscape) and “c” (discrimination by year, waterscape and month). Black vertical lines indicate the uncertainty when performing calculations using 25 and 75 percentiles instead of median values. Panel a) CO₂ flux, b) diffusive and c) total CH₄ flux. All fluxes are in GgC yr⁻¹. Bold y-axis labels indicate the calculation approach (case “c”) shown in more detail in Figure 5 for the individual contributions from rivers, channels and lakes.**

For the Danube Delta, CO₂ flux estimates decreased when considering spatial heterogeneity and seasonality, because the channel data, which showed the most pronounced seasonality and the highest fluxes, is treated independently and assigned to a comparably small area. Independent consideration of data from different years allows exploration of the inter-annual variability, which is quite pronounced for CO₂ (Fig. 7a). CH₄ emissions tend to be higher in 2017, but the trend is not as clear, especially considering total fluxes (Fig. 7c, case “b”). The lower CO₂ flux in 2017 can be explained by the weaker connection of the wetland to the freshwater system of the Danube. We expect that in 2017 most of the water exchange, especially during low discharge conditions, between the river and the inner delta was along the channels as surface water connections, with comparably little water laterally bypassing through the wetland. While the CO₂ fluxes from the river were only marginally smaller than in 2016, channels emitted less than 50 % and the lakes even turned into a net CO₂ sink in 2017 (Fig. 5a & 5b). The importance of flooded vegetated area on CO₂ concentration in rivers was also found in the Congo and Amazon river basins (Borges et al., 2015; Borges et al., 2019; Amaral et al., 2019), where larger inundated areas correlated with higher pCO₂ values. In the case of the lakes, reduced lateral inputs from adjacent wetlands reveal their large CO₂ uptake potential. However, this



525 might result in higher CH₄ emissions, as calculations according to case “b” indicate. Neglecting seasonality, diffusive CH₄ fluxes from the lakes were 0.3 GgC yr⁻¹ higher in 2017 (1.0 GgC yr⁻¹, data not shown).

Durisch-Kaiser et al. (2008) found Danube lakes to be sources of CO₂ and CH₄ to the atmosphere in both May and September 2006. Their measured fluxes fall well within the range of our observations. The comparison of data for corresponding months shows, however, that their CO₂ concentrations in May are on average twice as high as the ones we measured in 2016, while
530 September concentrations are on average 18 % smaller. The higher fluxes in May could have been due to the aftermath of the severe flood, which reached Romania in the second half of April 2006 and inundated large parts of the delta, thereby promoting lateral exchanges.

4.4 Lateral and atmospheric carbon fluxes

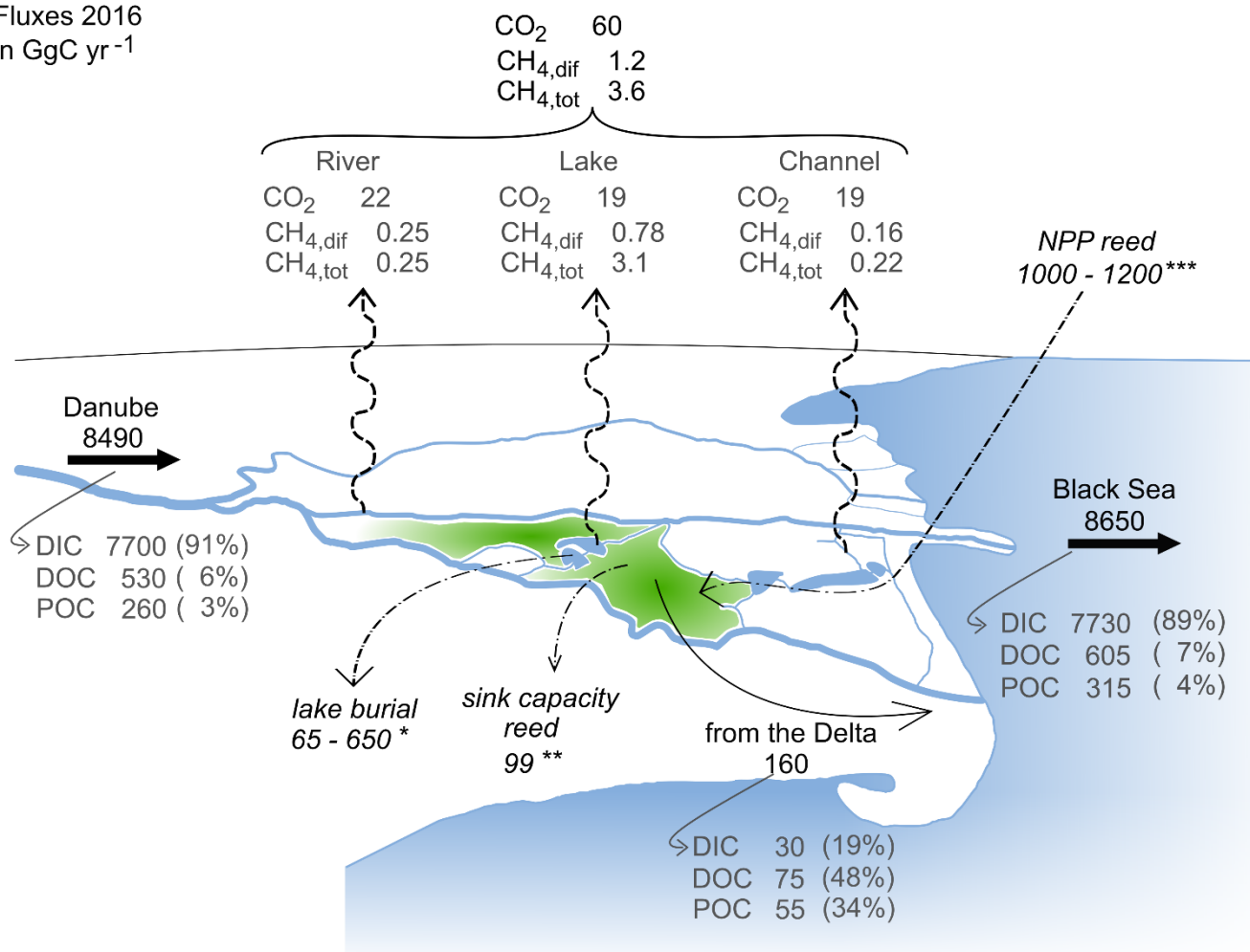
The freshwaters of the Danube Delta export in total about 225 GgC yr⁻¹ (Fig 8). About 40 % of this carbon is directly released
535 to the atmosphere, while 60 % of the carbon is transported laterally to the Danube and subsequently to the Black Sea. However, the majority of the carbon reaching the Black Sea originates from the catchment (8490 GgC yr⁻¹). The contribution from the delta is therefore comparably small and the fraction of dissolved and particulate carbon species is only marginally changed by the delta. The anthropogenic alterations of the river main branches, like the straightening and deepening to allow for commercial navigation, might be an explanation for this. Especially the Sulina and the St. George branch were strongly altered
540 in that respect, which has increased the discharge along these branches and decreased the lateral exchange with the delta. Excavation of the channels furthermore increased the surface water connection between different features of the delta.

Considering the area between the three main branches ($A_{\text{Delta}} = 3510 \text{ km}^2$, Table 1) and the catchment area ($A_{\text{catchment}} = 817000 \text{ km}^2$, Table 1), the deltaic carbon yield amounts to 46 gC m⁻² yr⁻¹, while the riverine carbon yield to the Black Sea is 11 gC m⁻² yr⁻¹. So although the Danube Delta contributes only about 2 % to the total carbon load reaching the
545 Black Sea, its role as a carbon source should not be underrated, as the carbon yield (net export/surface area) of the delta is about 4-fold higher than the yield of the overall catchment.

In total, the Danube River and its delta supplied the Black Sea with 8650 GgC yr⁻¹ in 2016, which fuels carbon emissions in the river plume. Based on concentration measurements in July 1995, Amouroux et al. (2002) estimated the CH₄ flux from the Danube River plume close to the St. George branch to 0.47 mmol m⁻² d⁻¹, which compares very well with the CH₄ flux we
550 measured in the Danube River branches. As CH₄ concentrations in the river plume were 5 to 10 times higher than in the rest of the water column, the authors expect this flux to be fueled by the carbon reaching the Black Sea from the delta. They estimate the total CH₄ emissions from river plumes in the Black Sea to be 28–52 GgC yr⁻¹, based on the total surface area of the plumes. Since the Danube River is providing more than 50 % of the total discharge and thus the largest freshwater contributor to the Black Sea (BSC, 2008), the majority of this emission might be released from the Danube River plume.
555 Assuming a share of 50 % of the total river plume emissions would mean that 8–16 % of the carbon laterally transported to the Black Sea might reach the atmosphere in the form of CH₄. This corresponds approximately to the share of DOC and POC transported to the Black Sea.



Fluxes 2016
 in GgC yr⁻¹



560 **Figure 8 Overview of carbon flux estimates in GgC yr⁻¹. The total area between the main branches is 3510 km² (see Table 1). Black and grey numbers refer to fluxes estimated during this study based on data from 2016. Italic values refer to estimates based on literature data: *carbon burial in lakes, based on average sedimentation rate measured in 7 lakes in the Danube Delta with an organic carbon content range of 3 – 30 % (Begy et al., 2018), ** sink capacity of *phragmites australis* upscaled to the area covered by scirpo-phragmitetum plant community (Zhou et al., 2009), *** upscaled net primary productivity of scirpo-phragmitetum plant community (Sarbu, 2006). The green area in the plot symbolizes the reed area without indicating all locations of its occurrence.**

565 The comparison of our lateral DOC and POC fluxes with available estimates of lateral carbon transport of European rivers to the ocean (Ludwig et al., 1996), indicates that about 3% and 4% of the POC and DOC could be exported by the Danube River alone. On a global scale, the lateral export of POC compares to the amount exported by the Zambezi River (Teodoru et al., 2015) but is about 20 % lower than the export from the Nile, despite the much higher discharge (Meybeck and Ragu, 1997). DOC export on the other hand is about twice as high in the Danube compared to Zambezi and Nile (Teodoru et al., 2015; Badr, 570 2016). The discharge of the Danube amounts to only 3 % of the discharge of the Amazon River, but it transports as much as 1/3 of the latter's DIC (Moquet et al., 2016; Druffel et al., 2005).



575 The CH₄ fluxes per unit area we observed in the Danube Delta were comparable with those of the Zambezi River but exceeded the fluxes of the Amazons' inner estuary reported by Sawakuchi et al. (2014). The CO₂ fluxes per unit area from the Danube are much smaller than the ones from the Amazon but are closer to those observed in the Mississippi, the Zambezi and the average deduced for estuarine systems (Jiang et al., 2019; Borges and Abril, 2011).

Table 3 Selected major rivers and their carbon fluxes to ocean and atmosphere.

River	Export to Ocean			water-air flux the from delta			
	[GgC yr ⁻¹]			[GgC yr ⁻¹]		[mmol m ⁻² d ⁻¹]	
	DOC	POC	DIC	CO ₂	CH ₄	CO ₂	CH ₄
Amazon	37600 ^a	6100 ^a	~24000 ^o – ~30000 ^p	28500 ^e	18.7 ^f	200–1470 ^e	0.38 ^f
Mississippi	930 ^l – 1900 ^c	1100 ^c – 3100 ^m	16000 ⁱ			55.5 ± 7.6 ⁱ	
Zambezi	263 ^b	306 ^b	3672 ^b	2731 ^b	48 ^b	58.9 ^b	1.03 ^b
Nile	300 ^{c, k}	400 ^c	12500 ^j				
Danube	605 ^q	315 ^q	7730 ^q	60 ^q	3.6 ^q	5.8–93 ^q	0.42–2.0 ^q
Global	200000 ⁿ – 240000 ^d	240000 ^d – 250000 ⁿ	410000 ^d – 450000 ⁿ	270000 ^{g, h}	709–1800 ^h	58 ^h	0.73–1.05 ^h

^a Coynel et al. (2005), ^b Teodoru et al. (2015), ^c Meybeck and Ragu (1997), ^d Li et al. (2017), ^e Sawakuchi et al. (2017), ^f flux from Sawakuchi et al. (2014), area for upscaling from Sawakuchi et al. (2017), ^g Laruelle et al. (2010), ^h Borges and Abril (2011), ⁱ Jiang et al. (2019) total DIC flux estimated using same discharge as ^c, ^j Soltan and Awadallah (1995) total flux estimated using same discharge as ^c, ^k Badr (2016) total flux estimated, ^l Bianchi et al. (2007), ^m Bianchi et al. (2004), ⁿ Kirschbaum et al. (2019), ^o Moquet et al. (2016) estimated from HCO₃⁻ flux, ^p Druffel et al. (2005) total flux estimated using same discharge as a, ^q this study

4.5 The role of the wetland

580 Based on a literature review, Cai (2011) suggested that estuarine CO₂ degassing is strongly supported by microbial decomposition of organic matter produced in adjacent coastal wetlands: while CO₂ produced in marsh areas and transported to the estuaries was lost to the atmosphere, riverine DIC and DOC content were not greatly altered. Also, several other studies highlight the impact of lateral input of wetlands or floodplain-derived water on river water O₂ content (Zurbrügg et al., 2012) and in-stream CO₂ levels ((D'Amario and Xenopoulos, 2015). Abril and Borges (2019) recently suggested that the active pipe concept of carbon transport in the aquatic continuum indeed needs to be extended to consider wetlands and dry land as separate



585 carbon sources. This is in agreement with the present study highlighting how exchange with the wetland can raise CO₂ fluxes well above locally sustained in-stream respiration. In the following, we therefore intend to identify and assess the potential role of the wetland in this complex hydrological system.

The Danube Delta is dominated by the plant association Scirpo-Phragmitetum, which covers nearly 89% of the total marsh area (1600 km²). Its net primary productivity ranges between 1500 to 1800 g m⁻² yr⁻¹ (Sarbu, 2006), which is slightly higher
590 than the average net primary productivity of intertidal salt marshes and mangroves (1275 gC m⁻² yr⁻¹) (Woodwell et al, 1973, Hopkinson 1988, as reported in (Cai, 2011)). Assuming a carbon content of 0.42 gC gBiomass⁻¹ determined by Greenway and Woolley (1999) for *Phragmites australis*, between 1000 and 1210 GgC yr⁻¹ are bound in the form of macrophyte biomass in the reed area of the Danube Delta. The wetlands thus hold 12 to 17 times the total input of organic C to the delta from the catchment. Most of the carbon is decomposed and released back to the atmosphere. Nevertheless, wetlands are considered to
595 be net C sinks and Zhou et al. (2009) estimate the sink capacity of a *Phragmites australis* dominated wetland to -62 gC m⁻² yr⁻¹ considering CO₂ and CH₄ release from the wetland itself. Scaled to the area of the Danube Delta, the potential sink of the wetland would amount to -99 GgC yr⁻¹. However, the study of Zhou et al. (2009) relied on eddy covariance measurements and did not take into account potential lateral export of carbon to adjacent water bodies. In the Mississippi Delta, DeLaune et al. (2018) found long-term storage of wetlands up to one order of magnitude lower than decadal carbon storage estimates. Assuming
600 that carbon emitted from the channels originated only from the wetland source, this would suggest that up to 20 % of the potential wetland sink might be exported laterally, eventually finding its way to the atmosphere.

Assessing the amount of carbon input needed to sustain the observed carbon fluxes in the delta by a simple mass balance approach shows that inputs need to be even higher (Eq. 7). For the mass balance, we consider the net export to the Danube River (F_{Danube} = 160 GgC yr⁻¹) and to the atmosphere (F_{atm} = 65 GgC yr⁻¹) and assume that sedimentation is predominantly
605 occurring in the lakes of the delta (F_{sedi}). Begy et al. (2018) found averaged sedimentation rates in the lakes of the delta in the range of 0.84 g cm⁻² yr⁻¹. Carbon content in the sediment cores ranged between 3–30 %, translating into a carbon burial rate of 65–650 GgC yr⁻¹ across all delta lakes. For the purpose of this simple balance, we neglect anthropogenic effects, e.g. removal of fish biomass or burning of the harvested reed areas during winter and potentially associated carbon inputs.

$$F_{\text{In}} \approx -F_{\text{Danube}} - F_{\text{atm}} - F_{\text{sedi}} \quad (7)$$
$$F_{\text{In}} \approx 290 \text{ to } 875 \text{ GgC yr}^{-1}$$

610

Assuming that freshwaters are a net balanced system and these three fluxes represent all major export fluxes suggests that an input of 290–875 GgC yr⁻¹ is required to sustain the export to the Danube, the atmosphere and the sediment. Since long-term carbon burial is most likely an order of magnitude smaller (DeLaune et al., 2018) than the decadal sedimentation rate we expect the required input to be rather at the lower end of the determined range. Nevertheless, it still surpasses the potential contribution
615 from the wetland as estimated above by a factor of 3. This might either indicate an underestimation of the lateral export from the wetland or significant contributions from other sources, such as the forest areas or anthropogenic inputs to the system from fish farms or wastewater. In addition, emergent macrophytes that border both lakes and channels in the delta could play an important role, since they fix carbon directly from the atmosphere but are decomposed in the water column.



5. Conclusions

620 The waterscapes in the Danube Delta differ significantly with respect to their carbon cycling. While the river is mainly
influenced by the carbon signal provided by the upstream catchment, carbon loads and especially greenhouse gas
concentrations in the channels are strongly affected by lateral inflow from adjacent wetlands. Local primary production and
respiration on the other hand dominate the carbon dynamics in the delta lakes. Considering the spatial extent of the three
different waterscapes and the seasonality of their effluxes, we estimate that 65 GgC yr⁻¹ were emitted from the delta to the
625 atmosphere in 2016. Considering the small surface area they cover (7 %), channels in general contributed disproportionately
to the total flux (30 %). Small lakes without direct connection to the main river could represent similar hotspots for greenhouse
gas evasion as the channels. Overall, nearly 8 % of the total flux to the atmosphere was released as CH₄, mostly supplied by
the lakes. Covering a full annual cycle and discriminating between the three dominant waterscapes of the delta, we reduce the
uncertainty linked to seasonal and spatial variability. However, spatial estimates could be further improved by investigating
630 the extent of hotspots, gradients between discrete sampling stations, the effect of more isolated lakes and channels of the delta
and the inter-annual variability, which especially CO₂ seems to show.

We estimate that the Danube Delta receives about 850 GgC yr⁻¹ from the upstream catchment. The export surpasses these
inputs with the net carbon source from the delta to the Black Sea amounting to about 160 GgC yr⁻¹. However, compared to the
overall carbon transfer from the Danube catchment (8490 GgC yr⁻¹) to the Black Sea, the contribution from the delta is about
635 2 % and will not significantly alter the bulk carbon composition of the river water. In terms of carbon yield, the contribution
from the delta is about 4-fold higher (45.6 gC m⁻² yr⁻¹) than the riverine carbon yield (10.6 gC m⁻² yr⁻¹).

In order to sustain the observed carbon fluxes from Danube Delta freshwaters to the atmosphere and the Black Sea while
assuming a net balanced system, a minimum of 290 GgC yr⁻¹ would be required to be provided by the wetland realm or other
sources within the Danube Delta.

640 Code availability

The Matlab scripts used for the calculations are available upon request.

Data availability

The data set with the measurements presented in this paper, as well as an accompanying metadata file have not been published
elsewhere and are available via the ETH Research Collection (<https://doi.org/10.3929/ethz-b-000416925>, Maier et al, 2020).

645 Sample availability

Not available



Video supplement

Not available

Supplement Link (Copernicus will include it)

650 Team list

Authors Contribution

BW and CT conceptualized the present study. CT led the monthly monitoring campaigns, supported by MSM. MSM was responsible for lab analysis of samples and subsequent data analysis. MSM prepared the figures and drafted both manuscript and supporting information. All authors engaged in discussing and editing the manuscript.

655 Competing interests

The authors declare that they have no conflict of interest.

Disclaimer

Acknowledgements

The authors thank Till Breitenmoser, Anna Canning, Christian Dinkel, Tim Kalvelage, Patrick Kathriner and Alexander
660 Mistretta for support during fieldwork and sample analysis in the lab. We also thank Scott Winton for his comments on the
manuscript. This work was supported by the Swiss State Secretariat for Education, Research and Innovation (SERI) under
contract number 15.0068. The opinions expressed and arguments employed herein do not necessarily reflect the official views
of the Swiss Government. The research leading to these results has received funding from the European Union's Horizon 2020
research and innovation program under the Marie Skłodowska-Curie grant agreement No 643052 (C-CASCADES project).
665 This product includes data licensed from International Commission for the Protection of the Danube River (ICPDR).

References

Abril, G., Martinez, J.-M., Artigas, L. F., Moreira-Turcq, P., Benedetti, M. F., Vidal, L., Meziante, T., Kim, J.-H., Bernardes,
M. C., Savoye, N., Deborde, J., Souza, E. L., Albéric, P., Landim de Souza, M. F., and Roland, F.: Amazon River carbon
dioxide outgassing fuelled by wetlands, *Nature*, 505, 395-398, 10.1038/nature12797, 2014.



- 670 Abril, G., and Borges, A. V.: Ideas and perspectives: Carbon leaks from flooded land: do we need to replumb the inland water active pipe?, *Biogeosciences*, 16, 769-784, 10.5194/bg-16-769-2019, 2019.
- Almeida, R. M., Pacheco, F. S., Barros, N., Rosi, E., and Roland, F.: Extreme floods increase CO₂ outgassing from a large Amazonian river, *Limnology and Oceanography*, 62, 989-999, 10.1002/lno.10480, 2017.
- Amaral, J. H. F., Farjalla, V. F., Melack, J. M., Kasper, D., Scofield, V., Barbosa, P. M., and Forsberg, B. R.: Seasonal and
675 spatial variability of CO₂ in aquatic environments of the central lowland Amazon basin, *Biogeochemistry*, 10.1007/s10533-019-00554-9, 2019.
- Amouroux, D., Roberts, G., Rapsomanikis, S., and Andreae, M. O.: Biogenic Gas (CH₄, N₂O, DMS) Emission to the Atmosphere from Near-shore and Shelf Waters of the North-western Black Sea, *Estuarine, Coastal and Shelf Science*, 54, 575-587, 10.1006/ecss.2000.0666, 2002.
- 680 Aufdenkampe, A. K., Mayorga, E., Raymond, P. A., Melack, J. M., Doney, S. C., Alin, S. R., Aalto, R. E., and Yoo, K.: Riverine coupling of biogeochemical cycles between land, oceans, and atmosphere, *Frontiers in Ecology and the Environment*, 9, 53-60, 2011.
- Badr, E.-S. A.: Spatio-temporal variability of dissolved organic nitrogen (DON), carbon (DOC), and nutrients in the Nile River, Egypt, *Environmental Monitoring and Assessment*, 188, 580, 10.1007/s10661-016-5588-5, 2016.
- 685 Begy, R. C., Simon, H., Kelemen, S., and Preoteasa, L.: Investigation of sedimentation rates and sediment dynamics in Danube Delta lake system (Romania) by ²¹⁰Pb dating method, *Journal of Environmental Radioactivity*, 192, 95-104, <https://doi.org/10.1016/j.jenvrad.2018.06.010>, 2018.
- Bianchi, T. S., Filley, T., Dria, K., and Hatcher, P. G.: Temporal variability in sources of dissolved organic carbon in the lower Mississippi river, *Geochimica et Cosmochimica Acta*, 68, 959-967, <https://doi.org/10.1016/j.gca.2003.07.011>, 2004.
- 690 Bianchi, T. S., Wysocki, L. A., Stewart, M., Filley, T. R., and McKee, B. A.: Temporal variability in terrestrially-derived sources of particulate organic carbon in the lower Mississippi River and its upper tributaries, *Geochimica et Cosmochimica Acta*, 71, 4425-4437, <https://doi.org/10.1016/j.gca.2007.07.011>, 2007.
- Borges, A. V.: Do we have enough pieces of the jigsaw to integrate CO₂ fluxes in the coastal ocean?, *Estuaries*, 28, 3-27, 10.1007/BF02732750, 2005.
- 695 Borges, A. V., Delille, B., and Frankignoulle, M.: Budgeting sinks and sources of CO₂ in the coastal ocean: Diversity of ecosystems counts, *Geophysical Research Letters*, 32, 10.1029/2005gl023053, 2005.
- Borges, A. V., and Abril, G.: Carbon Dioxide and Methane Dynamics in Estuaries, in: *Treatise on Estuarine and Coastal Science*, edited by: Wolanski, E., and McLusky, D., Academic Press, Waltham, 119-161, 2011.
- Borges, A. V., Abril, G., Darchambeau, F., Teodoru, C. R., Deborde, J., Vidal, L. O., Lambert, T., and Bouillon, S.: Divergent
700 biophysical controls of aquatic CO₂ and CH₄ in the World's two largest rivers, *Scientific Reports*, 5, 15614, 10.1038/srep15614
<https://www.nature.com/articles/srep15614#supplementary-information>, 2015.



- Borges, A. V., Darchambeau, F., Lambert, T., Morana, C., Allen, G. H., Tambwe, E., Sembaito, A. T., Mambo, T., Wabakhangazi, J. N., Descy, J. P., Teodoru, C. R., and Bouillon, S.: Variations in dissolved greenhouse gases (CO₂, CH₄, N₂O) in the Congo River network overwhelmingly driven by fluvial-wetland connectivity, *Biogeosciences*, 16, 3801-3834, 10.5194/bg-16-3801-2019, 2019.
- BSC: State of Environment of the Black Sea (2001-2006/7), Istanbul, Turkey, 448, 2008.
- Cai, W.-J.: Estuarine and Coastal Ocean Carbon Paradox: CO₂ Sinks or Sites of Terrestrial Carbon Incineration?, *Annual Review of Marine Science*, 3, 123-145, 10.1146/annurev-marine-120709-142723, 2011.
- 710 Cai, W. J., Arthur Chen, C. T., and Borges, A.: Carbon dioxide dynamics and fluxes in coastal waters influenced by river plumes, in: *Biogeochemical Dynamics at Major River-Coastal Interfaces: Linkages with Global Change*, edited by: Allison, M. A., Bianchi, T. S., and Cai, W.-J., Cambridge University Press, Cambridge, 155-173, 2013.
- Cole, J. J., Prairie, Y. T., Caraco, N. F., McDowell, W. H., Tranvik, L. J., Striegl, R. G., Duarte, C. M., Kortelainen, P., Downing, J. A., Middelburg, J. J., and Melack, J.: Plumbing the global carbon cycle: Integrating inland waters into the terrestrial carbon budget, *Ecosystems*, 10, 171-184, 10.1007/s10021-006-9013-8, 2007.
- 715 Coops, H., Hanganu, J., Tudor, M., and Oosterberg, W.: Classification of Danube Delta lakes based on aquatic vegetation and turbidity, in: *Biology, Ecology and Management of Aquatic Plants*, Springer, 187-191, 1999.
- Coops, H., Buijse, L. L., Buijse, A. D. T., Constantinescu, A., Covaliov, S., Hanganu, J., Ibelings, B. W., Menting, G., Navodaru, I., and Oosterberg, W.: Trophic gradients in a large-river Delta: ecological structure determined by connectivity gradients in the Danube Delta (Romania), *River Research and Applications*, 24, 698-709, 2008.
- 720 Coynel, A., Seyler, P., Etcheber, H., Meybeck, M., and Orange, D.: Spatial and seasonal dynamics of total suspended sediment and organic carbon species in the Congo River, *Global Biogeochemical Cycles*, 19, Artn Gb4019 10.1029/2004gb002335, 2005.
- D'Amario, S. C., and Xenopoulos, M. A.: Linking dissolved carbon dioxide to dissolved organic matter quality in streams, *Biogeochemistry*, 126, 99-114, 10.1007/s10533-015-0143-y, 2015.
- 725 Danube Commission: *Hydrologisches Nachschlagewerk der Donau 1921-2010*, Donaukommission Budapest, 2018.
- DaNUbs: *Nutrient Management in the Danube Basin and its Impact on the Black Sea*, Vienna University of Technology, 2005.
- De Muth, J. E.: *Basic Statistics and Pharmaceutical Statistical Applications*, 3rd Edition, Pharmacy Education Series, Hoboken Chapman and Hall/CRC, 2014.
- 730 DeLaune, R. D., White, J. R., Elsey-Quirk, T., Roberts, H. H., and Wang, D. Q.: Differences in long-term vs short-term carbon and nitrogen sequestration in a coastal river delta wetland: Implications for global budgets, *Organic Geochemistry*, 123, 67-73, <https://doi.org/10.1016/j.orggeochem.2018.06.007>, 2018.
- Drake, T. W., Raymond, P. A., and Spencer, R. G. M.: Terrestrial carbon inputs to inland waters: A current synthesis of estimates and uncertainty, *Limnology and Oceanography Letters*, 3, 132-142, 10.1002/lol2.10055, 2018.
- 735 Druffel, E. R. M., Bauer, J. E., and Griffin, S.: Input of particulate organic and dissolved inorganic carbon from the Amazon to the Atlantic Ocean, *Geochemistry, Geophysics, Geosystems*, 6, 10.1029/2004gc000842, 2005.



- Dubois, K. D., Lee, D., and Veizer, J.: Isotopic constraints on alkalinity, dissolved organic carbon, and atmospheric carbon dioxide fluxes in the Mississippi River, *Journal of Geophysical Research: Biogeosciences* (2005–2012), 115, 10.1029/2009JG001102, 2010.
- 740 Durisch-Kaiser, E., Pavel, A., Doberer, A., Reutimann, J., Balan, S., Sobek, S., Radan, S., and Wehrli, B.: Nutrient retention, total N and P export and greenhouse gas emission from the Danub Delta lakes, *GeoEcoMarina*, 14, 2008.
- Dürr, H. H., Laruelle, G. G., van Kempen, C. M., Slomp, C. P., Meybeck, M., and Middelkoop, H.: Worldwide Typology of Nearshore Coastal Systems: Defining the Estuarine Filter of River Inputs to the Oceans, *Estuaries and Coasts*, 34, 441–458, 10.1007/s12237-011-9381-y, 2011.
- 745 eDelta: <https://edelta.ro/isaccea-365>, 2017.
- Galloway, W. E.: Process framework for describing the morphologic and stratigraphic evolution of deltaic depositional systems, 1975.
- Greenway, M., and Woolley, A.: Constructed wetlands in Queensland: Performance efficiency and nutrient bioaccumulation, *Ecological Engineering*, 12, 39–55, [https://doi.org/10.1016/S0925-8574\(98\)00053-6](https://doi.org/10.1016/S0925-8574(98)00053-6), 1999.
- 750 Hedderich, J., and Sachs, L.: *Angewandte Statistik*, Springer, 2016.
- Holgerson, M. A., and Raymond, P. A.: Large contribution to inland water CO₂ and CH₄ emissions from very small ponds, *Nature Geosci*, advance online publication, 2016.
- Romanian National Institute of Hydrology and Water Management: http://www.inhga.ro/diagnoza_si_proгноza_dunare, access: 06.05.2019, 2017.
- 755 IPCC: The physical science basis. Contribution of working group I to the fourth assessment report of the Intergovernmental Panel on Climate Change, Cambridge University Press, Cambridge, United Kingdom and New York, NY, USA, 996, 2007, 2007.
- IPCC: Climate Change 2013: The Physical Science Basis. Contribution of Working Group I to the Fifth Assessment Report of the Intergovernmental Panel on Climate Change, Cambridge University Press, Cambridge; United Kingdom and New York, 760 NY; USA, 1535 pp., 2013.
- Irimus, I.: The hydrological regime of the Danube in the deltaic sector, in: *Danube Delta: genesis and biodiversity*, edited by: Tudorancea, C., and Tudorancea, M. M., Backhuys Publishers, Leiden, The Netherlands, 53–64, 2006.
- Jiang, Z.-P., Wei-Jun, C., Lehrter, J., Chen, B., Ouyang, Z., Le, C., Roberts, B. J., Hussain, N., Scaboo, M. K., and Zhang, J.: Spring net community production and its coupling with the CO₂ dynamics in the surface water of the northern Gulf of Mexico, 765 *Biogeosciences*, 16, 3507–3525, 2019.
- Kirschbaum, M. U. F., Zeng, G., Ximenes, F., Giltrap, D. L., and Zeldis, J. R.: Towards a more complete quantification of the global carbon cycle, *Biogeosciences*, 16, 831–846, 10.5194/bg-16-831-2019, 2019.
- Laruelle, G. G., Dürr, H. H., Slomp, C. P., and Borges, A. V.: Evaluation of sinks and sources of CO₂ in the global coastal ocean using a spatially-explicit typology of estuaries and continental shelves, *Geophysical Research Letters*, 37, 770 10.1029/2010gl043691, 2010.



- Lauerwald, R., Laruelle, G. G., Hartmann, J., Ciais, P., and Regnier, P. A. G.: Spatial patterns in CO₂ evasion from the global river network, *Global Biogeochemical Cycles*, 29, 534-554, doi:10.1002/2014GB004941, 2015.
- Li, M., Peng, C., Wang, M., Xue, W., Zhang, K., Wang, K., Shi, G., and Zhu, Q.: The carbon flux of global rivers: A re-evaluation of amount and spatial patterns, *Ecological Indicators*, 80, 40-51, <https://doi.org/10.1016/j.ecolind.2017.04.049>,
775 2017.
- Ludwig, W., Probst, J.-L., and Kempe, S.: Predicting the oceanic input of organic carbon by continental erosion, *Global Biogeochemical Cycles*, 10, 23-41, 10.1029/95gb02925, 1996.
<https://mapcruzin.com/free-romania-arcgis-maps-shapefiles.htm>, based on www.openstreetmap.org/, 2016a.
- Marchand, D., Prairie, Y. T., and Del Giorgio, P. A.: Linking forest fires to lake metabolism and carbon dioxide emissions in the boreal region of Northern Québec, *Global Change Biology*, 15, 2861-2873, 10.1111/j.1365-2486.2009.01979.x, 2009.
- Mayorga, E., Aufdenkampe, A. K., Masiello, C. A., Krusche, A. V., Hedges, J. I., Quay, P. D., Richey, J. E., and Brown, T. A.: Young organic matter as a source of carbon dioxide outgassing from Amazonian rivers, *Nature*, 436, 538-541, 2005.
- Meybeck, M., and Ragu, A.: River discharges to the oceans: an assessment of suspended solids, major ions and nutrients, UNEP, 1997.
- 785 Mihailescu, N.: Danube delta geology, geomorphology and geochemistry, in: *Danube Delta: Genesis and Biodiversity*, edited by: Tudorancea, C., and Tudorancea, M. M., Backhuys Publishers, Leiden, 9-35, 2006.
- Moquet, J. S., Guyot, J. L., Crave, A., Viers, J., Filizola, N., Martinez, J. M., Oliveira, T. C., Sanchez, L. S., Lagane, C., Casimiro, W. S., Noriega, L., and Pombosa, R.: Amazon River dissolved load: temporal dynamics and annual budget from the Andes to the ocean, *Environ Sci Pollut Res Int*, 23, 11405-11429, 10.1007/s11356-015-5503-6, 2016.
- 790 Niculescu, S., Lardeux, C., and Hanganu, J.: Alteration and Remediation of Coastal Wetland Ecosystems in the Danube Delta: A Remote-Sensing Approach, in: *Coastal Wetlands: Alteration and Remediation*, edited by: Finkl, C. W., and Makowski, C., Springer International Publishing, Cham, 513-553, 2017.
- Oosterberg, W., Staras, M., Bogdan, L., Buijse, A. D., Constantinescu, A., Coops, H., Hanganu, J., Ibelings, B. W., Menting, G. A. M., and Navodaru, I.: Ecological gradients in the Danube Delta lakes: present state and man-induced changes, 2000.
- 795 Pavel, A., Durisch-Kaiser, E., Balan, S., Radan, S., Sobek, S., and Wehrli, B.: Sources and emission of greenhouse gases in Danube Delta lakes, *Environmental Science and Pollution Research*, 16, 86-91, 2009.
- Postma, G.: An analysis of the variation in delta architecture, *Terra Nova*, 2, 124-130, 1990.
- Raymond, P. A., Hartmann, J., Lauerwald, R., Sobek, S., McDonald, C., Hoover, M., Butman, D., Striegl, R., Mayorga, E., Humborg, C., Kortelainen, P., Durr, H., Meybeck, M., Ciais, P., and Guth, P.: Global carbon dioxide emissions from inland
800 waters, *Nature*, 503, 355-359, 10.1038/nature12760, 2013.
- Regnier, P., Friedlingstein, P., Ciais, P., Mackenzie, F. T., Gruber, N., Janssens, I. A., Laruelle, G. G., Lauerwald, R., Luyssaert, S., Andersson, A. J., Arndt, S., Arnosti, C., Borges, A. V., Dale, A. W., Gallego-Sala, A., Goddérís, Y., Goossens, N., Hartmann, J., Heinze, C., Ilyina, T., Joos, F., LaRowe, D. E., Leifeld, J., Meysman, F. J. R., Munhoven, G., Raymond, P.



- A., Spahni, R., Suntharalingam, P., and Thullner, M.: Anthropogenic perturbation of the carbon fluxes from land to ocean, 805 Nat. Geosci., 6, 597, 10.1038/ngeo1830
<https://www.nature.com/articles/ngeo1830#supplementary-information>, 2013.
- Richey, J. E., Melack, J. M., Aufdenkampe, A. K., Ballester, V. M., and Hess, L. L.: Outgassing from Amazonian rivers and wetlands as a large tropical source of atmospheric CO₂, Nature, 416, 617-620, 10.1038/416617a, 2002.
- Sarbu, A.: Aquatic macrophytes, in: Danube Delta: Genesis and Biodiversity, edited by: Tudorancea, C., and Tudorancea, M. 810 M., Backhuys Publishers, Leiden, 133-175, 2006.
- Sawakuchi, H. O., Bastviken, D., Sawakuchi, A. O., Krusche, A. V., Ballester, M. V., and Richey, J. E.: Methane emissions from Amazonian Rivers and their contribution to the global methane budget, Global change biology, 20, 2829-2840, 2014.
- Sawakuchi, H. O., Neu, V., Ward, N. D., Barros, M. D. C., Valerio, A. M., Gagne-Maynard, W., Cunha, A. C., Less, D. F. S., Diniz, J. E. M., Brito, D. C., Krusche, A. V., and Richey, J. E.: Carbon Dioxide Emissions along the Lower Amazon River, 815 Frontiers in Marine Science, 4, UNSP 76
10.3389/fmars.2017.00076, 2017.
- Soltan, M., and Awadallah, R.: Chemical survey on the River Nile water from Aswan into the outlet, Journal of Environmental Science & Health Part A, 30, 1647-1658, 1995.
- Teodoru, C. R., Nyoni, F. C., Borges, A. V., Darchambeau, F., Nyambe, I., and Bouillon, S.: Dynamics of greenhouse gases 820 (CO₂, CH₄, N₂O) along the Zambezi River and major tributaries, and their importance in the riverine carbon budget, Biogeosciences, 12, 2431-2453, 2015.
- Tranvik, L. J., Downing, J. A., Cotner, J. B., Loiselle, S. A., Striegl, R. G., Ballatore, T. J., Dillon, P., Finlay, K., Fortino, K., and Knoll, L. B.: Lakes and reservoirs as regulators of carbon cycling and climate, Limnology and Oceanography, 54, 2298-2314, 2009.
- 825 Tudorancea, C., and Tudorancea, M. M.: Danube Delta: genesis and biodiversity, Backhuys Publishers, Leiden, 2006. Ecological Sciences for Sustainable Development. The Danube Delta.: <http://www.unesco.org/new/en/natural-sciences/environment/ecological-sciences/biosphere-reserves/europe-north-america/romaniaukraine/danube-delta/> access: 28.01.2019, 2019.
- Wanninkhof, R.: Relationship between wind speed and gas exchange over the ocean, Journal of Geophysical Research: Oceans, 830 97, 7373-7382, doi:10.1029/92JC00188, 1992.
- Ward, N. D., Sawakuchi, H. O., Neu, V., Less, D. F. S., Valerio, A. M., Cunha, A. C., Kampel, M., Bianchi, T. S., Krusche, A. V., Richey, J. E., and Keil, R. G.: Velocity-amplified microbial respiration rates in the lower Amazon River, Limnology and Oceanography Letters, 3, 265-274, doi:10.1002/lol2.10062, 2018.
- Weiss, R. F.: Carbon dioxide in water and seawater: the solubility of a non-ideal gas, Marine Chemistry, 2, 203-215, 835 [https://doi.org/10.1016/0304-4203\(74\)90015-2](https://doi.org/10.1016/0304-4203(74)90015-2), 1974.



Zhang, K., Liu, Y., Chen, Q., Luo, H., Zhu, Z., Chen, W., Chen, J., and Mo, Y.: Effect of submerged plant species on CH₄ flux and methanogenic community dynamics in a full-scale constructed wetland, *Ecological Engineering*, 115, 96-104, <https://doi.org/10.1016/j.ecoleng.2018.02.025>, 2018.

840 Zhou, L., Zhou, G., and Jia, Q.: Annual cycle of CO₂ exchange over a reed (*Phragmites australis*) wetland in Northeast China, *Aquatic Botany*, 91, 91-98, <https://doi.org/10.1016/j.aquabot.2009.03.002>, 2009.

Zurbrügg, R., Wamulume, J., Kamanga, R., Wehrl, B., and Senn, D. B.: River-floodplain exchange and its effects on the fluvial oxygen regime in a large tropical river system (Kafue Flats, Zambia), *Journal of Geophysical Research: Biogeosciences*, 117, doi:10.1029/2011JG001853, 2012.

845